We thank the editor for his positive comments on our revised manuscript and the opportunity to clarify better the potential role of pH for the considered chemical and biological processes. We made the following changes in the main text of manuscript and the supplemental information (editor comment in green, *all manuscript in italics, new text in blue*).

*Thank you for submitting your revised manuscript. You have largely addressed the major comments and questions from the referees. However, it seems that you have made very few and small revisions regarding the important series of questions from Referee 1 regarding the importance of pH in the chemistry you are studying and modeling. While you provide an often extensive response to the referee, few changes to the actual manuscript were made regarding this important topic. For example, it will not be clear to most readers that the pH was strongly buffered and likely did not change, or that you have reason to believe that most of the reactions and processes you are considering are not very pH dependent. Furthermore, a clear justification for the use of pH 7 buffer when cloud water is more acidic (pH 3-6) should be provided, along with a discussion of why you think it is reasonable to use a pH of 4 in the model while a pH of 7 was used in the experiments.*

We addressed this comment in multiple sections in detail below. In addition, we would like to point that we realized that the figure caption of Figure 3 was wrongly formatted. We corrected it in the revised version.

Regarding the experimental conditions, we added the following text **in Section 2.1.1 (Cell preparation for further incubation)**

> *Bacteria pellets were rinsed first with 5 mL of NaCl 0.8% and after with Volvic® mineral water (pH = 7.0), previously sterilized by filtration under sterile conditions using a 0.22 µm PES filter. The pH value was fairly stable during the incubations because of the presence of carbonates in Volvic® mineral water, which buffer the system, and because no acids were formed as products of the biotransformation of phenol and catechol.*

In addition, we added **in Section 3.1 (Incubation in microcosms):**

> *The transformation rates described in this work were measured at pH = 7.0 which ~~which does not correspond to the whole range of~~ is within the range of pHs encountered in real clouds as observed at the Puy de Dome (3.8 < pH < 7.6, Deguillaume et al, 2014), but we expect that our results can be extrapolated to the full range of pH values as encountered in clouds. In our previous studies, we have demonstrated that pH variation has a low impact on microbial biodegradation ability as it was shown in the case of carboxylic acids by 17 strains isolated from clouds (Vaïtilingom et al., 2011) or phenol by Pseudomonas aeruginosa (Razika, et al., 2010). This insensitivity to the solution pH can be explained by the fact that the biodegradation experiments are performed with bacteria and not purified enzymes. The enzymatic activities take place inside the cell and are not impacted by the external pH. It is well known that bacteria are able to regulate their internal pH (which is usually in the range of ~6.5 < pH < ~7 when exposed to external pHs between 4 and 8. Yeasts, molds or acidophilic and alcalinophilic bacteria are even active in arrange of pH from 2 < pH < 11 (Beales, 2004). The mechanisms involved in the intracellular pH regulation of microorganisms facing acid stress are very complex and have been reviewed recently (Guan and Liu, 2020).*

In order to compare the contributions of chemical reactions in the gas and aqueous phases to the microbial processes in the aqueous phase only, we compare the rates of the loss processes of phenol and catechol. We modified the text **at the beginning of Section 2.3.1**:

*We use a multiphase box model to compare the loss ~~reactions~~ rates of phenol and catechol in the gas and aqueous phases by radicals (•OH, $NO_3$•) in both phases and bacteria only in the aqueous phase over a processing time of 15 min to simulate chemical and biological processing in a single cloud cycle. For each set of processes (•OH/$NO_3$•, phenol/catechol), the three terms in the following equation are calculated and the relative importance of each process is determined*

$$\frac{d[Aromatic]}{dt}\left[\frac{molec}{cm^3_{gas}\,s}\right] = \underbrace{-k_{chem,gas}\,[Radical(gas)][Aromatic(gas)]}_{loss\ by\ gas\ phase\ chemistry}$$

$$-\left[\underbrace{k_{chem,aq}\,[Radical(aq)][Aromatic(aq)]}_{loss\ by\ aqueous\ phase\ chemistry} + \underbrace{k_{bact,aq}\,[Cell][Aromatic(aq)]}_{\substack{loss\ by\ microbial\ processes\\ in\ the\ aqueous\ phase}}\right] LWC\ N_A\ 0.001$$

*(Eq-2)*

*whereas [Aromatic] denotes the phenol or catechol concentration, [Radical] the •OH or $NO_3$• concentration in the gas or aqueous phase, respectively, and $k_{chem,gas}$, $k_{chem,aq}$ and $k_{bact}$ are the rate constants as listed in Table S-1 in the Supporting Information. The units of the aqueous phase processes are converted into the same units as the gas phase processes (molec $cm^{-3}$ $s^{-1}$) with LWC (= liquid water content = 9.7 $\cdot 10^{-7}$ L(aq)/L(gas)), $N_A$ = 6.022 $\cdot 10^{23}$ molecules/mol (Avogadro constant) and 0.001 to convert from L to $cm^3$.*

*The pH value of cloud water is assumed to be constant (pH = 4), to represent conditions of a continental, moderately polluted cloud. It should be pointed out that the choice of the pH value in the simulations does not affect the results as for a wide range of pH values (3 < pH < 6) – being typical for clouds influenced by marine and continental air masses (Deguillaume et al., 2014). None of the parameters in Eq-2 is pH dependent within the range relevant for cloud water (cf Section S 3-3).*

In addition, we consider the phase transfer processes of the radicals and aromatics between the gas and aqueous phases, described using the resistance model (Schwartz, 1986) which is commonly used in multiphase model applications, using Henry's law constants $K_H$, mass accommodation coefficients $\alpha$ and gas phase diffusion coefficients $D_g$ (Table S-1).

Only if any of the phase transfer parameters or rate constants were pH dependent, the individual rates in Eq-2 would show different values for different pH values. We added a new **Section S 3-3 in the supporting information** to give the reasoning for the assumption of pH independence for all of these parameters within the pH range commonly found for cloud water:

It can be expected that none of the rates in Eq-2 shows any significant dependence on cloud relevant pH values due to the following reasoning:

**$k_{chem,gas}$:** The gas phase rate constants describe chemical processes in the gas phase and, thus, are intendent of any solution properties, such as pH.

**$k_{chem,aq}$:** The rate constants of $NO_3$ and OH reactions with the phenolic aromatics are not expected to show any pH dependence since the reactions occur via H-abstraction and thus the rate constants are a function of the bond strength of the hydrogen bonds (e.g. discussion in (Herrmann, 2003)). Even though the rate constant of $NO_3$ and OH with phenol and catechol have not been investigated as a function of pH, the small variability of rate constants of other alcohols (e.g. NIST solution data base), suggests that our assumption of a pH-independent $k_{chem,aq}$ is reasonable. Only if the pH value increases to very high pH values, i.e. near the acid dissociation values of phenols ($pK_a$ ~ 10), differences in the reaction mechanisms (e.g. electron transfer) and, thus, in rate constants may be expected.

**$k_{bact,aq}$:** We have shown in previous studies that the biodegradation rates for several organics and bacteria strains do not show any systematic dependence on pH within a range of ~5 < pH < ~6.3 (Vaïtilingom et al., 2011). This insensitivity to the surrounding solution pH is expected: Unlike chemical reactions, the biodegradation does not occur in the surrounding water phase, but within the bacteria cells which self-regulate their pH values to a range of 6.5-7, even if the surrounding pH varies over wide ranges. Only at very acidic (pH < 2) or very alkaline (pH > 10) solutions, the internally buffered pH value within the cells might be different.

**[Radical]:** For both radicals, OH and $NO_3$, the main source in the aqueous phase is the direct uptake from the gas phase, e.g. (Ervens et al., 2003; Tilgner et al., 2013). Since gas phase processes are independent of pH, the radical gas phase concentration is not affected by the solution pH. Other source processes of the OH(aq) radical include aqueous phase reactions, such as the direct photolysis of $H_2O_2$ or Fenton reactions (reactions of iron(II) with hydroperoxides), which also do not show any pH dependence over the range of relevant values (~2< pH < ~7)

**[Aromatic]:** The concentrations of the aromatics are initial values of the model. Given that [Aromatic] is included in all three terms in Eq-R1, they cancel anyway in the comparison of the three terms for a given simulation.

**$K_H$:** Henry's laws constants for the radicals or aromatics, respectively, do not show any pH dependence. Admittedly, there are only very few pH dependent measurements available for these and related compounds. However, since Henry's law

Only at very high pH values, i.e. near the pKa values of the phenols (pH ~ 10), the effective Henry's law constants for the aromatics maybe higher than the physical Henry's law constants. As pH value of cloud water is significantly below this threshold, it is safe to neglect this dissociation.

**$\alpha$:** The mass accommodation coefficient describes the probability of a molecule to 'stick' on a surface upon collision. There is no physical reason why this process should pH dependent and no data that corroborate such a dependency.

**$D_g$:** Gas phase diffusion is a process that occurs only in the gas phase and thus is independent of any solution properties (including pH).

**References**

Beales, N.: Adaptation of Microorganisms to Cold Temperatures, Weak Acid Preservatives, Low pH, and Osmotic Stress: A Review, Comprehensive Reviews in Food Science and Food Safety, 3(1), 1–20, doi:10.1111/j.1541-4337.2004.tb00057.x, 2004.

Deguillaume, L., Charbouillot, T., Joly, M., Vaïtilingom, M., Parazols, M., Marinoni, A., Amato, P., Delort, A. M., Vinatier, V., Flossmann, A., Chaumerliac, N., Pichon, J. M., Houdier, S., Laj, P., Sellegri, K., Colomb, A., Brigante, M. and Mailhot, G.: Classification of clouds sampled at the puy de Dôme (France) based on 10 yr of monitoring of their physicochemical properties, Atmos. Chem. Phys., 14(3), 1485–1506, doi:10.5194/acp-14-1485-2014, 2014.

Ervens, B., George, C., Williams, J. E., Buxton, G. V., Salmon, G. A., Bydder, M., Wilkinson, F., Dentener, F., Mirabel, P., Wolke, R. and Herrmann, H.: CAPRAM2.4 (MODAC mechanism): An extended and condensed tropospheric aqueous phase mechanism and its application, J. Geophys. Res., 108(D14), 4426, doi:doi: 10.1029/2002JD002202, 2003.

Guan, N. and Liu, L.: Microbial response to acid stress: mechanisms and applications, Applied Microbiology and Biotechnology, 104(1), 51–65, doi:10.1007/s00253-019-10226-1, 2020.

Herrmann, H.: Kinetics of aqueous phase reactions relevant for atmospheric chemistry, Chem. Rev., 103(12), 4691–4716, 2003.

Razika, B., Abbes, C., Messaoud, C. and Soufi, K.: Phenol and Benzoic Acid Degradation by Pseudomonas aeruginosa, Journal of Water Resource and Protection, 2(9), 788–791, 2010.

Schwartz, S.: Mass transport considerations pertinent to aqueous phase reactions of gases in liquid water clouds, in Chemistry of Multiphase Atmospheric Systems, vol. 6, edited by W. Jaeschke, pp. 415–471, Springer, Berlin., 1986.

Tilgner, A., Bräuer, P., Wolke, R. and Herrmann, H.: Modelling multiphase chemistry in deliquescent aerosols and clouds using CAPRAM3.0i, J Atmos Chem, 70(3), 221–256, doi:10.1007/s10874-013-9267-4, 2013.

Vaïtilingom, M., Charbouillot, T., Deguillaume, L., Maisonobe, R., Parazols, M., Amato, P., Sancelme, M. and Delort, A. M.: Atmospheric chemistry of carboxylic acids: microbial implication versus photochemistry, Atmos. Chem. Phys., 11(16), 8721–8733, doi:10.5194/acp-11-8721-2011, 2011.

# Biodegradation of phenol and catechol in cloud water: Comparison to chemical oxidation in the atmospheric multiphase system

Saly Jaber[1], Audrey Lallement[1], Martine Sancelme[1], Martin Leremboure[1], Gilles Mailhot[1], Barbara Ervens[1*] and Anne-Marie Delort[1*]

[1]Université Clermont Auvergne, CNRS, SIGMA Clermont, Institut de Chimie de Clermont-Ferrand, F-63000 Clermont-Ferrand, France

*Correspondence to:* Anne-Marie Delort (a-marie.delort@uca.fr) and Barbara Ervens (barbara.ervens@uca.fr)

**Abstract**

The sinks of hydrocarbons in the atmosphere are usually described by oxidation reactions in the gas and aqueous (cloud) phases. Previous lab studies suggest that in addition to chemical processes, biodegradation by bacteria might also contribute to the loss of organics in clouds; however, due to the lack of comprehensive data sets on such biodegradation processes, they are not commonly included in atmospheric models. In the current study, we measured the biodegradation rates of phenol and catechol, which are known pollutants, by one of the most active strains selected during our previous screening in clouds (*Rhodococcus enclensis*). For catechol, biodegradation transformation is about ten times faster than for phenol. The experimentally derived biodegradation rates are included in a multiphase box model to compare the chemical loss rates of phenol and catechol in both the gas and aqueous phases to their biodegradation rate in the aqueous phase under atmospheric conditions. Model results show that the degradation rates in the aqueous phase by chemical and biological processes for both compounds are similar to each other. During daytime, biodegradation of catechol is even predicted to exceed the chemical activity in the aqueous phase and to represent a significant sink (17%) of total catechol in the atmospheric multiphase system. In general, our results suggest that atmospheric multiphase models may be incomplete for highly soluble organics as biodegradation may represent an unrecognized efficient loss of such organics in cloud water.

## 1. Introduction

Monocyclic aromatic compounds in the atmosphere are of great interest due to their influence on ozone formation (Hsieh et al., 1999) and their potential to form secondary organic aerosol (Ng et al., 2007). Their main sources include combustion processes of coal, oil and gasoline. Substituted monocyclic aromatics are semivolatile and partition between the atmospheric gas and particulate phases. Among those, phenol is of particular interest for air quality as it is considered one of the main pollutants listed by U.S Environmental Protection Agency (US EPA list) since it represents a risk for both humans and the environmental biota (TOXNET Toxicology Data Network, 2019). Measurements of gas phase mixing ratios of phenol in the atmosphere are sparse. The few available measurements show rather low values with 4 - 40 ppt at the continental site Great Dun Fell (Lüttke and Levsen, 1997), and 0.4 ppt, 2.6 ppt and 2.7 ppt at suburban, rural and urban locations (Delhomme et al., 2010), respectively. However, phenol's much higher water-solubility ($K_H$ = 647 M atm$^{-1}$) as compared to benzene ($K_H$ ~ 0.2 M atm$^{-1}$) leads to nanomolar levels in cloud water (5.5 – 7.7 nM at the puy de Dôme (France) (Lebedev et al., 2018), 30 – 95 nM at Great Dun Fell (Lüttke et al., 1997), and 37 nM in the Vosges Mountains (Levsen et al., 1993)). The further hydroxylated catechol is even less volatile and more water-soluble and, based on its Henry's law constant of $K_H = 8.3 \cdot 10^5$ M atm$^{-1}$, expected to be nearly fully dissolved (> 80%) in cloud water, which might explain the lack of its detection in the gas phase. Phenolic compounds have been shown to comprise 2 - 4% of the total organic particulate matter at several locations at the Northeastern US (Bahadur et al., 2010). In the same study, a strong correlation between seawater-derived organics and phenolic compounds was found, which suggests direct sources in addition to hydroxylation of the unsubstituted aromatics.

The oxidation of phenol by $^{\bullet}$OH radicals leads to catechol in the gas (Xu and Wang, 2013), the aqueous (Hoffmann et al., 2018) phases and at the gas/aqueous interface (Pillar et al., 2014); further $^{\bullet}$OH oxidation of catechol leads to ring-opening products. A recent multiphase model study suggests that the main aqueous phase loss processes of aromatics with two hydroxyl groups include not only $^{\bullet}$OH and $NO_3^{\bullet}$ reactions in clouds but also reactions with $O_3$ and $HO_2^{\bullet}$ (Hoffmann et al., 2018). The nitration of phenols represents the major atmospheric source of nitrophenols in the gas phase (Yuan et al., 2016) and aqueous phase (Harrison et al., 2005; Vione et al., 2003). Nitrophenols can be phytotoxic (Harrison et al., 2005) and also contribute to light-absorption of atmospheric particles ('brown carbon' (Xie et al., 2017)). They have been found in atmospheric particles (Chow et al., 2016) and in the aqueous phases of clouds, fog and lakes (Lebedev et al., 2018). In addition, phenols add to secondary organic aerosol formation in the aqueous phase by oligomerization reactions (Yu et al., 2014).

Not only chemical reactions, but also microbial processes in the aqueous phase of clouds act as sinks for organic compounds (Delort et al., 2010). Biodegradation rates for several bacteria strains and aliphatic mono- and dicarboxylic acids/carboxylates as well as for formaldehyde and methanol (Ariya et al., 2002; Fankhauser et al., 2019; Husárová et al., 2011; Vaïtilingom et al., 2010, 2011, 2013) have been measured

in laboratory experiments. Comparison of such rates to those of chemical radical ($^{\bullet}OH$ or $NO_3^{\bullet}$) reactions in the aqueous phase show comparable rates of chemical and microbial processes under atmospherically relevant conditions. Such a comparison has not been performed yet for phenolic compounds in the aqueous phase due to the lack of data on their biodegradation rates.

Our previous metagenomic and metatranscriptomic study, directly performed on cloud water samples collected at the puy de Dôme station in France, showed convincing evidence of the in-cloud expression of genes coding for enzymes involved in phenol biodegradation (Lallement et al., 2018b). We found transcripts for phenol monooxygenases and phenol hydroxylases responsible for the hydroxylation of phenol into catechol and transcripts for catechol 1,2-dioxygenases leading to the opening of the aromatic ring. These genes originated from the genera *Acinetobacter* and *Pseudomonas* belonging to Gamma-proteobacteria, a major class of bacteria in clouds (Lallement et al., 2018b). In the same study, a large screening of bacteria in parallel isolated from cloud water samples (*Pseudomonas* spp., *Rhodococcus* spp. and strains from the Moraxellaceae family) showed that 93% of the strains could biodegrade phenol. Altogether, these results indicate a high potential of cloud microorganisms to biotransform phenol and catechol in cloud water.

In the current study, we designed lab experiments in microcosms mimicking cloud water conditions in terms of light, bacteria and temperature. Under these conditions, we measured the biodegradation rates of phenol and catechol by *Rhodococcus enclensis* PDD-23b-28, isolated from cloud water and one of the most efficient strains able to degrade phenol during our previous screening (Lallement et al., 2018b). The derived biodegradation rates for *Rhodococcus*, together with literature data on phenol and catechol biodegradation by *Pseudomonas*, were implemented in a box model to compare chemical and microbial degradation rates in the atmospheric multiphase system.

## 2. Materials and Methods

### 2.1 Experiments in microcosms

The transformation rates of phenol and catechol were measured in microcosms mimicking cloud water conditions at the puy de Dôme station (1465 m). Solar light was fitted to that measured directly under cloudy conditions (*Figure S-1*); 17°C is the average temperature in the summer at this location. *Rhodococcus* bacterial strains belong to the most abundant bacteria in cloud waters and are very active phenol biodegraders (Lallement et al., 2018b; Vaïtilingom et al., 2012). Fe(EDDS) was used to mimic organic ligands of Fe(III), in particular siderophores (Vinatier et al., 2016). In addition, This complex is stable at the working pH of 6.0 (Li et al., 2010).

#### 2.1.1. Cell preparation for further incubations

*Rhodococcus enclensis PDD-23b-28* was grown in 25 mL of R2A medium for 48 h at 17°C, 130 rpm (Reasoner and Geldreich, 1985). Then cultures were centrifuged at 4000 rpm for 15 min at 4°C. Bacteria

pellets were rinsed first with 5 mL of NaCl 0.8% and after with Volvic® mineral water (pH = 7.0), previously sterilized by filtration under sterile conditions using a 0.22 µm PES filter. The bacterial cell concentration was estimated by optical density at 600 nm using a spectrophotometer UV3100 to obtain a concentration close to $10^9$ cell $mL^{-1}$. Finally, the concentration of cells was precisely determined by counting the colonies on R2A Petri dishes.

### 2.1.2. Phenol transformation

**Biotransformation:** *Rhodococcus enclensis PDD-23b-28* cells were re-suspended in 5 mL of 0.1 mM phenol (Fluka > 99%) solution, prepared in Volvic® mineral water, and incubated at 17°C, 130 rpm agitation for 48 hours in the dark. 0.5 mL of this culture was incubated in 25 mL of the same medium and under the same conditions. In order to determine the concentration, the optical density for each strain was measured at 600 nm during the experiment. The strain concentration was ~$10^9$ cells $mL^{-1}$. The concentration ratio of bacterial cells to phenol was kept similar to that as measured in cloud water (Lallement et al., 2018b). We showed in the past that in repeated experiments identical cell / substrate ratios lead to the same biodegradation rates (Vaïtilingom et al., 2010).

A control experiment was performed by incubating phenol without bacteria; phenol concentration remained stable over time (0.1 mM of phenol was obtained at the end of the experiment). For phenol quantification over time in the incubation experiments, 600 µL samples were centrifuged at 12500 rpm for 3 min and the supernatants were kept frozen until HPLC analysis. Complementary experiments were also performed consisting of incubation of the cells and 0.1 mM phenol in the presence of light without Fe(EDDS).

***Phototransformation:*** A 0.1 mM phenol solution (Fluka > 99%), prepared in Volvic® mineral water, was incubated at 17°C, 130 rpm agitation for 48 hours in photo-bioreactors designed by Vaïitilingom et al (2011). OH radicals were generated by photolysis adding 0.5 mM Fe(EDDS) complex solution. The Fe(EDDS) solution (iron complex with 1:1 stoichiometry) was prepared from iron(III) chloride hexahydrate ($FeCl_3$, $6H_2O$; Sigma-Aldrich) and (S,S)-ethylenediamine-N,N'-disuccinic acid trisodium salt (EDDS, 35% in water). A complementary experiment was also performed consisting of incubation of a 0.1 mM phenol solution in the presence of light without Fe(EDDS) complex.

The experimental conditions of the irradiation experiments (Sylvania Reptistar lamps; 15 W; 6500 K) are described by Wirgot et al (2017). They are mimicking the solar light measured under cloudy conditions at the puy de Dôme station (***Figure S-1***). The mechanism of the $^{\bullet}OH$ radical production under light irradiation is as follows (Brigante and Mailhot, 2015):

$$\text{Fe(III)-EDDS} \xrightarrow{h\nu} \text{[Fe(III)-EDDS]*} \longrightarrow \text{Fe(II)} + \text{EDDS}^{\bullet} \quad \text{(R-1)}$$

$$\text{EDDS}^{\bullet} + O_2 \longrightarrow O_2^{\bullet -} + \text{EDDS}_{ox} \quad \text{(R-2)}$$

$$HO_2 \rightleftharpoons O_2^- + H^+ \quad \text{(R-3)}$$

$$HO_2^{\bullet} + O_2^{\bullet-} \xrightarrow{H^+} H_2O_2 + O_2 + {}^{-}OH \quad \text{(R-4)}$$

$$HO_2^{\bullet} + HO^{\bullet}{}_2 \xrightarrow{H^+} H_2O_2 + O_2 \quad \text{(R-5)}$$

$$Fe(III) + O_2^{\bullet-} \longrightarrow Fe(II) + O_2 \quad \text{(R-6)}$$

$$Fe(III) + HO_2^{\bullet} \longrightarrow Fe(II) + O_2 + H^+ \quad \text{(R-7)}$$

$$Fe(II) + H_2O_2 \longrightarrow Fe(III) + {}^{\bullet}OH + {}^{-}OH \quad \text{(R-8)}$$

Using the specifications of the lamp, an overall rate constant of the photolysis of the Fe(III)-EDDS complex $j_{R\text{-}8} = 1.4 \cdot 10^{-3}$ $s^{-1}$ was calculated (***Section S-2***).

$$Fe(III)\text{-EDDS} \xrightarrow{h\nu} {}^{\bullet}OH + \text{products} \quad \text{(R-9)}$$

Assuming steady-state conditions for $^{\bullet}OH$ at the beginning of the experiments (i.e., equal $^{\bullet}OH$ production and loss rates), an $^{\bullet}OH$ concentration of $8.3 \cdot 10^{-13}$ M can be calculated. This concentration is at the upper limit of $^{\bullet}OH$ concentrations as derived from various measurements and model studies (Arakaki et al., 2013; Lallement et al., 2018a).

***Photo-biotransformation:*** The protocols for biotransformation and photo-transformation of phenol in the presence of Fe(EDDS) as described above were combined.

### 2.1.3. Catechol transformation

***Biotransformation:*** As for phenol, *Rhodococcus enclensis PDD-23b-28* cells were re-suspended in 5 mL of 0.1 mM catechol (Fluka > 99%) solution, prepared in Volvic® mineral water, and incubated at 17°C, 130 rpm agitation for 48 hours in the dark. Four experiments were carried out with different cell concentrations ($10^9$ cell $mL^{-1}$, $10^8$ cell $mL^{-1}$, $10^7$ cell $mL^{-1}$ and $10^6$ cell $mL^{-1}$). For catechol quantification over time in the incubation experiments, 600 µL samples were centrifuged at 12500 rpm for 3 min and the supernatants were kept frozen until LC-HRMS analysis.

## 2.2 Analytical methods

### 2.2.1. Phenol HPLC analysis

Before analysis, all samples were filtered on H-PTFE filter (pore size at 0.2 µm and diameter of 13 mm from Macherey-Nagel, Germany). Phenol detection was done on HPLC VWR Hitachi Chromaster apparatus fitted with a DAD detector and driven by Chromaster software. Isocratic mode was used with a reverse phase end-capped column (LiChrospher® RP-18, 150 mm x 4.6 mm, 5 µm, 100 Å). The mobile phase was composed of acetonitrile and filtered water (Durapore® membrane filters, 0.45 µm HVLP type, Ireland) in 25/75 ratio with a flow rate at 1.2 mL $min^{-1}$. Sample injection volume was 50 µL, spectra were recorded at 272 nm and the run time was 10 min.

### 2.2.2. Catechol LC-HRMS Analyses

LC-HRMS analyses of catechol were performed using an RSLCnano UltiMate™ 3000 (Thermo Scientific™) UHPLC equipped with an Q Exactive™ Plus Hybrid Quadrupole-Orbitrap™ Mass Spectrometer (Thermo Scientific™) ionization chamber. The same conditions were used for analyzing EDDS. Chromatographic separation of the analytes was performed on a Kinetex® EVO C18 (1.7 µm, 100 mm × 2.1 mm, Phenomenex) column with column temperature of 30°C. The mobile phases consisted of 0.1% formic acid and water (A) and 0.1% formic acid and acetonitrile (B). A three-step linear gradient of 95% A and 5% B in 7.5 min, 1% A and 99% B in 1 min, 95% A and 5% B for 2.5 min was used throughout the analysis. This device was associated with a Thermo Scientific™ Dionex™ UltiMate™ DAD 3000 detector (200-400 nm).

The Q-Exactive ion source was equipped with a electrospray ionization (ESI) and the Q-Orbitrap™. The Q-Exactive was operated in either full MS-SIM, the full MS scan range was set from m/z 80 to 1200. The mass resolution was set to 70000 fwhm, and the instrument was tuned for maximum ion throughput. AGC (automatic gain control) target or the number of ions to fill C-Trap was set to $10^6$ with a maximum injection time (IT) of 50 ms. The C-Trap is used to store ions and then transfer them to the Orbitrap mass analyzer. Other Q-Exactive generic parameters were: gas ($N_2$) flow rate set at 10 a.u., sheath gas ($N_2$) flow rate set at 50 a.u., sweep gas flow rate set at 60 a.u., spray voltage at 3.2 kV in positive mode, and 3 kV in negative mode, capillary temperature at 320°C, and heater temperature at 400°C. Analysis and visualization of the data set were performed using Xcalibur™ 2.2 software from Thermo Scientific™.

### 2.2.3. Derivation of phenol and catechol degradation rates

The degradation rates of phenol and catechol were calculated after normalization based on the ratio of the concentration at time t (C) and the concentration at time t = 0 ($C_0$). The pseudo-first-order rate constants ($k_{phenol}$ and $k_{catechol}$) were determined using ***Equation 1***:

$$\ln(C/C_0) = f(t) = - k_{phenol} \text{ (or } k_{catechol}) \, t \qquad \text{(Eq-1)}$$

## 2.3 Description of the multiphase box model

### 2.3.1. Chemical and biological processes

We use a multiphase box model to compare the loss ~~reactions~~ rates of phenol and catechol in the gas and aqueous phases by radicals ($^{\bullet}OH$, $NO_3^{\bullet}$) in both phases and bacteria only in the aqueous phase over a processing time of 15 min to simulate chemical and biological processing in a single cloud cycle. For each set of processes ($^{\bullet}OH/NO_3^{\bullet}$, phenol/catechol), the three terms in the following equation are calculated and the relative importance of each process is determined

$$\frac{d[\text{Aromatic}]}{dt}\left[\frac{\text{molec}}{\text{cm}^3_{\text{gas}}\,\text{s}}\right] = \underbrace{-k_{\text{chem,gas}}\,[\text{Radical(gas)}][\text{Aromatic(gas)}]}_{\text{loss by gas phase chemistry}}$$

$$-\left[\underbrace{k_{chem,aq}\,[Radical(aq)][Aromatic(aq)]}_{\text{loss by aqueous phase chemistry}} + \underbrace{k_{bact,aq}\,[Cell][Aromatic(aq)]}_{\text{loss by microbial processes in the aqueous phase}}\right] LWC\ N_A\ 0.001 \quad \text{(Eq-2)}$$

whereas [Aromatic] denotes the phenol or catechol concentration, [Radical] the •OH or $NO_3$• concentration in the gas or aqueous phase, respectively, and $k_{chem,gas}$, $k_{chem,aq}$ and $k_{bact}$ are the rate constants as listed in Table S-1 in the Supporting Information. The units of the aqueous phase processes are converted into the same units as the gas phase processes (molec $cm^{-3}$ $s^{-1}$) with LWC (= liquid water content = 9.7 $\cdot 10^{-7}$ L(aq)/L(gas)), $N_A$ = 6.022 $\cdot 10^{23}$ molecules/mol (Avogadro constant) and 0.001 to convert from L to $cm^3$.

The pH value of cloud water is assumed to be constant (pH = 4), to represent conditions of a continental, moderately polluted cloud. It should be pointed out that the choice of the pH value in the simulations does not affect the results as for a wide range of pH values (3 < pH < 6) – being typical for clouds influenced by marine and continental air masses (Deguillaume et al., 2014). None of the parameters in Eq-2 is pH dependent within the range relevant for cloud water (cf Section S 3-3). In addition to the data for *Rhodococcus* obtained in the current study, we also include literature data on the biodegradation of phenol and catechol by *Pseudonomas putida* and *Pseudonomas aeruginosa* (Section 3.2), which are usually more abundant in the atmosphere than *Rhodococcus*.

The processes considered in the gas and aqueous phases are summarized in ***Table S-1*** and ***Figure 1***. In both phases, the reaction of phenol with •OH is assumed to yield 50% catechol; other products of these reactions are not further tracked in the model. The reaction of phenol with $NO_3$• results in nitrophenols

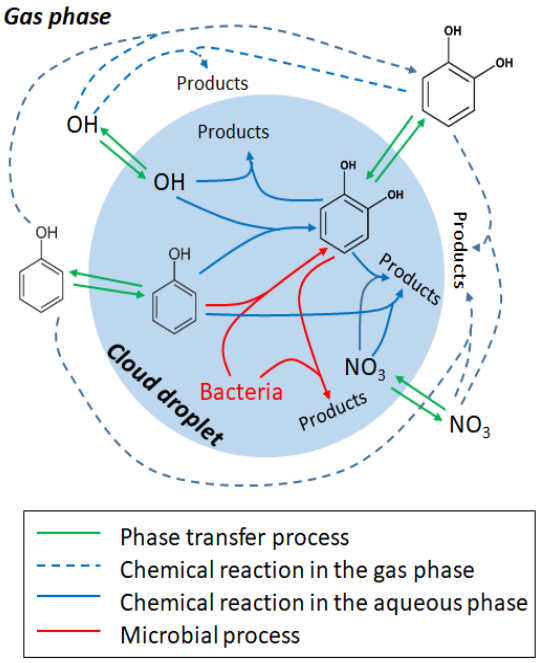


***Figure 1:*** *Schematic of the multiphase system in the box model*

(Bolzacchini et al., 2001; Harrison et al., 2005); the loss of these products is not explicitly included in the model either as we solely focus on the comparison of the degradation rates. Recently, it was suggested that the reactions with ozone and $HO_2^{\bullet}/O_2^{\bullet-}$ might represent major sinks (~50% and ~20%, respectively) of catechol in the aqueous phase (Hoffmann et al., 2018). However, the only available rate constant for the ozone reaction was derived at pH = 1.5 by Gurol and Nekouinaini (1984) who postulate that at higher pH (~5 - 6), the reaction with OH likely dominates the overall loss. Therefore, in our base case simulations, we limit the reactions of phenol and catechol to the reactions with $^{\bullet}OH$ and $NO_3^{\bullet}$ radicals. Sensitivity studies including the $HO_2^{\bullet}/O_2^{\bullet-}$ and $O_3$ reactions are discussed in the supporting information (***Section S-4***).

Microbial activity in the aqueous phase by *Rhodococcus* and *Pseudonomas* is usually expressed as rates [mol $cell^{-1}$ $h^{-1}$] (Vaïtilingom et al., 2013). We converted these experimentally-derived rates into 'rate constants' [L $cell^{-1}$ $h^{-1}$] in order to adjust them to the substrate and cell concentrations as assumed in the aqueous phase in the model (***Section S-3.2***), equivalent to the treatment of chemical processes. In order to account for the numerous additional loss processes of $^{\bullet}OH(aq)$ and $NO_3^{\bullet}(aq)$ in clouds, sinks for both radicals have been added: A general rate constant of OH with total water-soluble organic carbon (WSOC) ($k_{OH,WSOC} = 3.8 \cdot 10^8$ $M^{-1}$ $s^{-1}$) lumps the main loss processes of OH in cloud water (Arakaki et al., 2013); assuming an average WSOC concentration of 5 mM results in a first-order loss process of $k_{OH} = 2 \cdot 10^6$ $s^{-1}$. The main losses of $NO_3^{\bullet}(aq)$ are likely reactions with halides (Herrmann et al., 2000); as a proxy, we assume here a first-order loss process ($k_{NO3} = 10^5$ $s^{-1}$), reflecting the sum of the major $NO_3^{\bullet}(aq)$ sinks. These lumped sink processes lead to aqueous phase radical concentrations of $[^{\bullet}OH(aq)]_{day} \sim 10^{-15}$ M and $[NO_3^{\bullet}(aq)]_{night} \sim 10^{-14}$ M, respectively, in agreement with predictions from previous model studies (Ervens et al., 2003). Kinetic phase transfer processes between the two phases are described for the radicals and aromatics based on the resistance model by Schwartz (1986); all phase transfer parameters (Henry's law constants $K_H$, mass accommodation coefficients $\alpha$ and gas phase diffusion coefficients $D_g$) are summarized in ***Table S-1***.

### 2.3.2. Initial concentrations

Initial concentrations of 4 ppt catechol and phenol are assumed in the gas phase that partition between both phases and are chemically consumed over the course of the simulation (15 min). These initial mixing ratios correspond to equivalent aerosol mass concentrations on the order of several 10s ng $m^{-3}$, in agreement with measurements of phenol compounds in aerosol samples (Bahadur et al., 2010; Delhomme et al., 2010) and nanomolar concentrations in cloud water (Lebedev et al., 2018). It should be noted that the assumption on the initial aromatic concentrations does not affect any conclusions of our model studies, as we compare the loss fluxes of all processes in a relative sense. Two simulations are performed for each set of conditions to simulate day or night time conditions, respectively, that only differ by the radical concentrations ($[^{\bullet}OH]_{day} = 5 \cdot 10^6$ $cm^{-3}$; $[NO_3^{\bullet}]_{night} = 5 \cdot 10^8$ $cm^{-3}$) that are constant throughout the simulations. Two types of bacteria are assumed (*Rhodococcus* and *Pseudomonas*). They

have been found to contribute to 3.6% and 19.5% to the total number concentration of bacteria cells isolated from cloud waters and present in our lab collection. Using a typical cell concentration in cloud water of $6.8 \cdot 10^7$ cell $L^{-1}$(Amato et al., 2017), the assumed bacteria cell concentrations in the model are $2.7 \cdot 10^6$ cell $L^{-1}$ and $1.3 \cdot 10^7$ cell $L^{-1}$ for *Rhodococcus* and *Pseudomonas*, respectively. The simulations are performed for the conditions for monodisperse droplets with a diameter of 20 µm. The drop number concentration of 220 $cm^{-3}$ results in a total liquid water content of 0.9 g $m^{-3}$. These parameters do not change over the course of the simulation.

## 3. Results

### 3.1 Incubations in microcosms

The transformation rates described in this work were measured at pH = 7.0 ~~which does not correspond to the whole range of pHs encountered in real clouds~~ as observed at the Puy de Dome (3.8 < pH < 7.6, Deguillaume et al, 2014). , but we expect that our results can be extrapolated to the full range of pH values as encountered in clouds. In our previous studies, we have demonstrated that pH variation has a low impact on microbial biodegradation ability as it was shown in the case of carboxylic acids by 17 strains isolated from clouds (Vaïtilingom et al., 2011) or phenol by Pseudomonas aeruginosa (Razika, et al., 2010). This insensitivity to the solution pH can be explained by the fact that the biodegradation experiments are performed with bacteria and not purified enzymes. The enzymatic activities take place inside the cell and are not impacted by the external pH. It is well known that bacteria are able to regulate their internal pH (which is usually in the range of ~6.5 < pH < ~7 when exposed to external pHs between 4 and 8. Yeasts, molds or acidophilic and alcalinophilic bacteria are even active in arrange of pH from 2 < pH < 11 (Beales, 2004). The mechanisms involved in the intracellular pH regulation of microorganisms facing acid stress are very complex and have been reviewed recently (Guan and Liu, 2020).~~However, bacteria are able to control their intracellular pH under such conditions, and it has been shown that pH variation has a low impact on their biodegradation ability (Vaitilingom et al. 2011; Razika et al. 2010).~~

#### 3.1.1. Transformation of phenol

***Abiotic degradation*:** In the presence of light and Fe(EDDS), phenol concentration decreases with time in the first two hours of the experiments and then remains rather stable (***Figure 2***). In parallel, catechol, the first intermediate of phenol transformation is formed (***Figure S-2A***) and accumulates over time. Catechol concentration is quite low because it is further oxidized over time to yield $CO_2$. Phenol degradation slows down after two hours due to the lack of OH radical production resulting from the destruction of the EDDS ligand with time (***Figure S-2B***). Phenol is not directly photolyzed in the presence of light while it is oxidized in the presence of Fe(EDDS) complex (***Figure 2 and Figure S-2***).

***Biotic degradation*:** In the dark, phenol is biotransformed by *Rhodococcus enclensis* cells (***Figure 2***) and completely degraded after 5.5 hours. A lag time of about 2.5 hours is observed, during which phenol is degraded extremely slowly. This is a well-known phenomenon under lab conditions corresponding to the induction period of the gene expression (Al-Khalid and El-Naas, 2012). Catechol is slowly formed in parallel until t = 3.5 hours and is further biodegraded when bacteria have started to be more active (***Figure S-2A***).

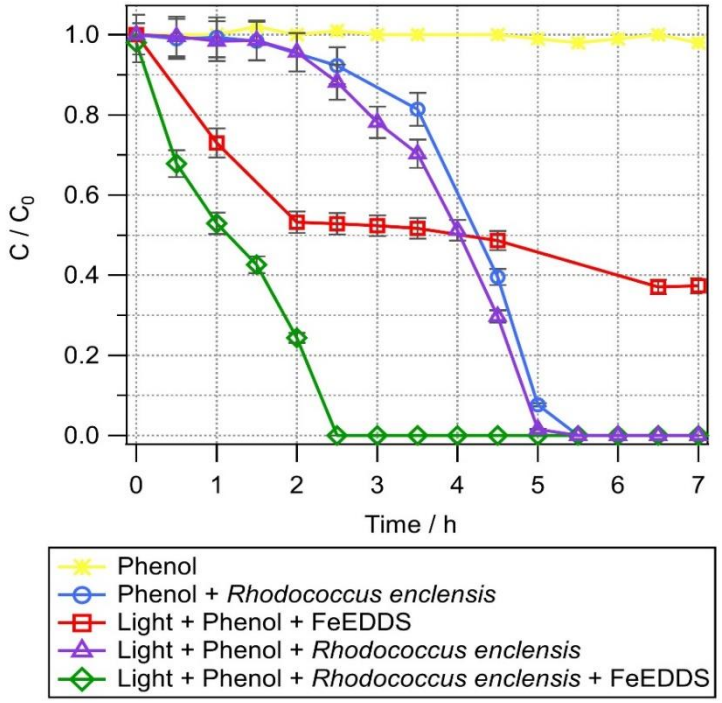


***Figure 2:*** *Transformation of phenol with time under different conditions. Phenol+Light +Fe(EDDS) (red squares), Phenol+ R.enclensis +dark (blue circles), Phenol+R. enclensis +Light (purple triangles), Phenol+ R. enclensis +Light + Fe(EDDS) (green line). Rhodococcus enclensis cell concentration was* $10^9$ *cells* $mL^{-1}$.

***Abiotic and biotic combined transformation*:** When light (in the absence of Fe(EDDS)) is present no major change is observed for the biodegradation of phenol by *Rhodococcus enclensis* (***Figure 2***); the lag time is still observed. When light and Fe(EDDS) are present, the lag time is no longer observed and the degradation of phenol is completed within 2.5 hours instead of 5.5 hours when the bacteria are in the dark. The microbial activity compensates the limitation of radical processes due to the destruction of the Fe(EDDS) complex (after two hours). In parallel, the production of catechol is increased compared to biotic or abiotic conditions alone (Figure S-2A). Catechol accumulates over approximately three hours; after which it decreases. As observed previously, this decrease is likely a result of the bacterial activity.

***Comparison of the rates of phenol transformation under the different conditions:*** If we consider the numerous uncertainties, the rates of transformation under abiotic, biotic and combined conditions are

within the same order of magnitude, namely ~$10^{-5}$ mol $L^{-1}$ $h^{-1}$ (***Table 1***). Biotic and combined conditions can be further compared in more detail by normalizing the transformation rates with the exact number of cells present in the different incubations (three biological replicates for each condition). Note that the number of cells varied from $4 \cdot 10^8$ to $8 \cdot 10^9$ cell $mL^{-1}$. After normalisation to the cell concentration used in the individual experiments, it is evident that the rates of phenol transformation are very close to each other and in the range of $10^{-16}$ mol $cell^{-1}$ $h^{-1}$ (***Table 2***).

***Table 1:*** *Transformation rates [$10^{-5}$ mol $L^{-1}$ $h^{-1}$] of catechol and phenol under abiotic and biotic conditions. The rates were measured from three biological or chemical replicates (independent experiments), respectively. They were derived based on the steepest slopes in Figure 2.*

| Phenol Light + Fe(EDDS) | Phenol *Rhodococcus enclensis* (dark) | Phenol *Rhodococcus enclensis* + Light | Phenol *Rhodococcus enclensis* Light + Fe(EDDS) | Catechol *Rhodococcus enclensis* (dark) |
|---|---|---|---|---|
| 3.1 ± 0.9 | 14 ± 6.4 | 4.7 ± 3.2 | 5.7 ± 0.5 | 15 ± 0.5 |

### 3.1.2. Biotransformation of catechol

As catechol is an intermediate of phenol transformation, we measured its biotransformation rate by *Rhodococcus enclensis* under dark conditions. When the cell concentration was $10^8$ or $10^9$ cell $mL^{-1}$, the catechol biodegradation was too fast to be detected within the time resolution of the experiments (Figure 3). We performed various experiments with reduced cell concentrations, from $10^7$ cell $mL^{-1}$ to $10^6$ cell $mL^{-1}$ (Figure 3). Finally, we used the results corresponding to $10^7$ cell $mL^{-1}$ to derive the initial rate of catechol biotransformation. It was estimated as $(15 \pm 0.5) \cdot 10^{-16}$ mol $cell^{-1}$ $h^{-1}$. This value is 8.5 times higher than the biodegradation rate of phenol and was used in the model (***Section 3.2***).

Straube (1987) showed that the activity of the catechol-1, 2-dioxygenase of *Rhodococcus* sp P1 was higher than that of its phenol hydroxylase. This trend is in agreement with our results as we know from the genome sequencing of our *Rhodococcus enclensis* strain that a catechol-1,2-dioxygenase is involved (and not a catechol-2,3-dioxygenase) (Lallement et al., 2017). As opposed to the results for phenol in Figure 2, it can be seen in Figure 3 that no lag time is observed for catechol biodegradation. This suggests

that the first step of oxidation of phenol to catechol by a phenol hydroxylase might be a limiting step as it needs to be induced, while the second step -corresponding to the opening of the ring cycle by a catechol-dioxygenase - is not induced and, thus, faster.

## 3.2 Comparison of biodegradation rates by *Rhodococcus* to literature data for *Pseudomonas* strains

As we previously have shown that *Pseudomonas* is one of the most dominant and active genus in cloud

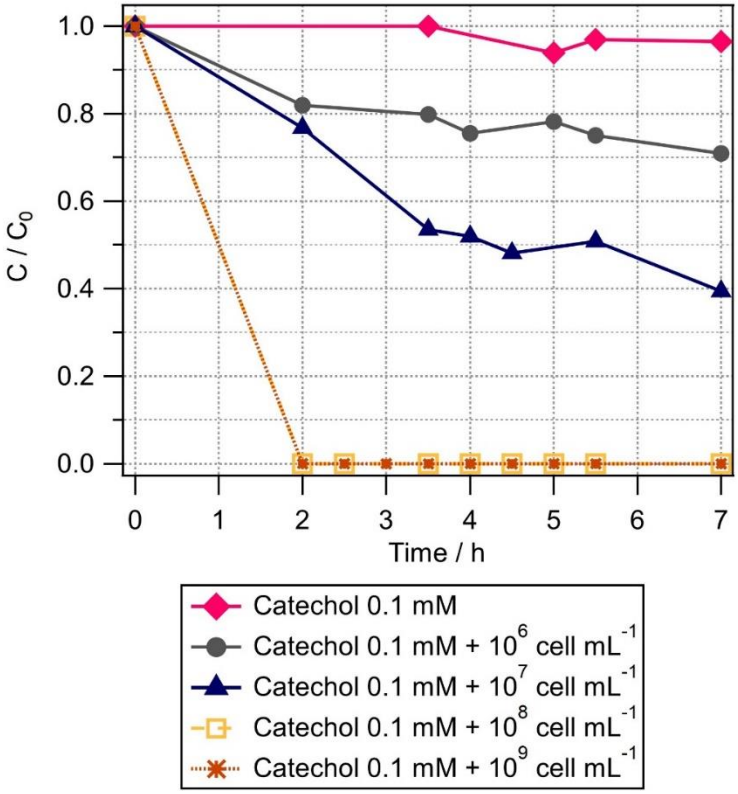


***Figure 32:*** *Biotransformation of catechol with time by different concentrations of Rhodococcus enclensis: $10^9$ cell $mL^{-1}$ (brown stars), $10^8$ cell $mL^{-1}$ (brown squares), $10^7$ cell $mL^{-1}$ (blue triangles) , $10^6$ cell $mL^{-1}$ (black circles). C = phenol concentration at time t, $C_0$ = initial phenol concentration, $C/C_0$ was extrapolated from the ratio of the integrals of the catechol signal m/z = 110.03678 detected in mass spectra at time t = 0 and t, respectively. Initial catechol concentration was 0.1 mM.* ~~***Figure 3:*** *Transformation of phenol with time under different conditions. Phenol+Light +Fe(EDDS) (red*~~

waters (Amato et al., 2019) and that these strains are very active for phenol biodegradation (Lallement et al., 2018b and references therein), we compare in the following biodegradation rates of *Pseudomonas* from the literature (Table 2) to the data for *Rhodococcus* derived in the current study (Section 4). These rates differ for among *Pseudomonas* strains: for *Pseudomonas putida* EKII a value of $0.199 \cdot 10^{-16}$ mol $cell^{-1}$ $h^{-1}$ was found (Hinteregger et al., 1992), while it was $5.89 \cdot 10^{-16}$ mol $cell^{-1}$ $h^{-1}$ for *Pseudomonas aeruginosa* (Razika et al., 2010b). Theses values are both on the same order of magnitude as the one measured here for *Rhodococcus enclensis PDD-23b-28.* Finally, we used an average value ($3.044 \cdot 10^{-16}$ mol $cell^{-1}$ $h^{-1}$) for *Pseudomonas* strains to derive the rates used in the model (***Section S-3.2***).

***Table 2**: Biodegradation rates [mol cell$^{-1}$ h$^{-1}$] of catechol and phenol of Rhodococcus and Pseudomonas strains normalized to the exact number of cells present in the incubations. The calculation of biodegradation rates for the Pseudomonas strains are detailed in S-1.*

| **Bacterial strain (experimental condition)** | **Biodegradation rate of phenol ($10^{-16}$ mol cell$^{-1}$ h$^{-1}$)** | **Biodegradation rate of catechol ($10^{-16}$ mol cell$^{-1}$ h$^{-1}$)** | **References** |
|---|---|---|---|
| *Rhodococcus enclensis PDD-23b-28 (dark)* | 1.8 ± 0.5 | 15.0 ± 0.5 | This work |
| *Rhodococcus enclensis PDD-23b-28 (light)* | 1.2 ± 0.5 | ND[1)] | This work |
| *Rhodococcus enclensis PDD-23b-28 (light+Fe(EDDS))* | 1.0 ± 0.3 | ND[1)] | This work |
| *Pseudomonas putida EKII (dark)* | 0.2 | 2.4 | (Hinteregger et al., 1992) |
| *Pseudomonas aeruginosa (dark)* | 5.9 | 70.7[2)] | Phenol experiments (Razika et al., 2010b) |
| *Pseudomonas (average)* | **Average: 3.0** | **Average: 36.6** | |

*[1)] Not determined; [2)] This rate was estimated based on the value for phenol (Razika et al., 2010) and the ratio (~ 12) for phenol/catechol biodegradation rates as determined for Pseudomonas putida by Hinteregger et al. (1992) (cf also Section 1-1 in the supplement)*

As in the case of phenol, we also calculated catechol biodegradation rates with *Pseudomonas strains* based on literature data (***Table 2***). Values are only available for *Pseudomonas putida* EKII (Hinteregger et al., 1992) and show a biodegradation rate that is twelve times higher compared to that of phenol biodegradation. This confirms that catechol dioxygenases are much more active than phenol hydroxylases as observed for *Rhodococcus enclensis*. Similar to phenol, catechol biodegradation rates for *Pseudomonas* are within the same order of magnitude as those for *Rhodococcus*. The same ratio (~12) as for the *Pseudomonas putida* was applied to estimate the biodegradation rate of catechol by *Pseudomonas aeruginosa*, for which only the rate for phenol was experimentally determined by Razika et al. (2010).

### 3.3 Model results

Model results are expressed as the relative contributions of each loss pathway in the gas and aqueous phases; they are summarized in ***Table S-4***. Both during day and night, the gas phase reactions of $^{\bullet}$OH and $NO_3^{\bullet}$ dominate the loss of phenol by > 99% (light red and blue bars in ***Figure 4a*** and ***b***, respectively). The contributions of *Pseudomonas* to the phenol loss are approximately a factor of three higher than those of *Rhodococcus,* in accordance with their higher cell concentration and comparable microbial activity (***Table S-3***). However, during daytime, the contribution of bacteria to the total loss in the aqueous phase is about one order of magnitude smaller than that of the chemical ($^{\bullet}$OH(aq)) reactions; during night-time, this difference is even larger and the $NO_3^{\bullet}$(aq) reactions dominate by far (factor > 100) the loss in the aqueous phase (***Figure 4b***).

While the microbial activity is the same during day and night time (i.e. there were no significant differences in experiments with and without light, respectively; ***Figure 2***), the night-time $NO_3^{\bullet}$(aq) concentration is about ten times higher (~$10^{-14}$ M) than that of $^{\bullet}$OH(aq) (~$10^{-15}$ M) during the day, and while the chemical rate constants also differ by a factor of four ($k_{OH,phenol}$ = $1.9 \cdot 10^9$ $M^{-1}$ $s^{-1}$; $k_{NO3,Phenol}$ = $8.4 \cdot 10^9$ $M^{-1}$ $s^{-1}$, Table S-1). These differences in radical concentrations and rate constants lead to much higher radical reaction rates during night than during the day and, thus, to a relatively lower importance of microbial activity during night time. Overall, the loss in the aqueous phase by both chemical and microbial processes contributes to ~ 0.1% to the total loss of phenol during night-time.

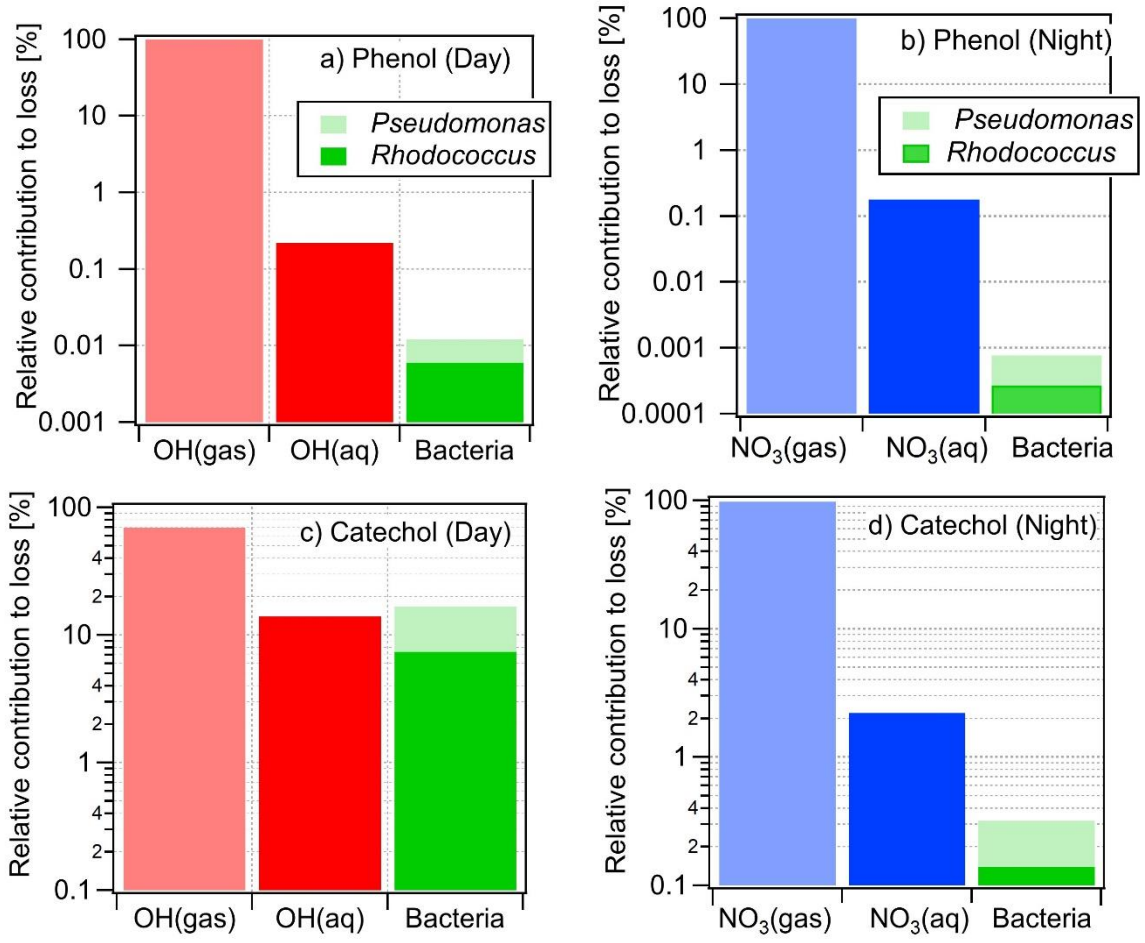


***Figure 3*** *: Relative contributions of multiphase processes to total loss of phenol (a, b) and catechol (c, d) during day (a, c) and night (b, d) time. Loss by bacteria processes only occur in the aqueous phase. Note that the ordinate is shown as a logarithmic scale which might falsely lead to the impression of larger contributions of Rhodococcus compared to Pseudomonas.*

The catechol fraction dissolved in the aqueous phase is much greater (≥ 85%) as its Henry's law constant is about 1000 times larger than that of phenol (***Table S-1***) of which only ~2% partition to the aqueous phase. Its enhanced solubility leads to a more important role of aqueous phase processes. During daytime, the loss by aqueous phase processes (chemical and microbial) is >30% for catechol (***Figure 4c***), with contributions by $^{\bullet}$OH(aq), *Pseudomonas* and *Rhodococcus* of 14%, 10% and 7%, respectively, when OH as the only oxidant for the phenols in the aqueous phase is considered. Thus, for this case, the

total microbial activity in the aqueous exceeds that of the chemical reactions (***Figure 4c***) and contributes to up to 17% to the total loss of catechol in the multiphase system. The relative higher gas phase rate constants and $NO_3^{\bullet}$ concentrations as compared to the corresponding values for $^{\bullet}OH$ during daytime, is reflected in the much higher contributions by the gas phase reactions to catechol loss during night (> 97%) than during daytime (***Figure 4d***).

The model results in ***Figure 4*** imply that the only chemical loss reactions of phenol and catechol are the reactions with the $^{\bullet}OH$ and $NO_3^{\bullet}$ radicals. In agreement with findings from a recent multiphase modeling study that discussed possible contributions of aqueous phase reactions with additional oxidants ($O_3$ and $HO_2^{\bullet}/O_2^{\bullet-}$) (Hoffmann et al., 2018), we show that including these reactions might add significant sinks for catechol (***Section S-4***). However, we caution that these results of the model sensitivity study including the ozone and $HO_2/O_2^-$ reactions likely represent an upper estimate The rate constant used in the model was determined at pH = 1.5. In the original study, a decreasing trend with increasing pH was suggested; however, the exact pH dependence was not given. Thus, the prediction shown in Figure S-3 might not correspond to the moderate pH values as encountered in clouds and thus might be an overestimate of the role of the ozone reaction. .

## 4. Atmospheric implications

Both experimental and modelling approaches show that, in the water phase of clouds, suggest that phenol and catechol degradation by microbial and chemical OH(aq) processes may be within one order of magnitude. When the complete multiphase system is taken into account, phenol chemical transformation is largely dominant in the gas phase whereas the more water-soluble catechol is efficiently biodegraded in the aqueous phase.

Our estimates are only based on a limited number of cloud microorganisms (*Pseudomonas* and *Rhodococcus*). These microorganisms represent strains which are very efficient and previous works showed that these genera are active in clouds (Amato et al., 2017; Lallement et al., 2018b). However, they only comprise a fraction of the total microfora, i.e. about 22% of all prokaryotes in clouds. Even if other bacterial genera are less metabolically active, their combined metabolic activity might contribute substantially to the total biodegradation of phenols (and likely other water-soluble organics) in clouds. In addition, other microorganisms could be active as well, such as fungi and yeasts. The relative importance of radical chemistry compared to biodegradation will also depend on the radical concentrations in both phases which, in turn, are a function of numerous factors such as air mass characteristics, pollution levels that affect OH concentrations and microphysical cloud properties (e.g., drop diameters, liquid water content) (Ervens et al., 2014). In general, the importance of aqueous phase processes increases with increasing solubility (Henry's law constants). Our recent cloud FT-ICR-MS analyses of cloud water samples have shown that about 50% of ~2100 identified compounds were utilized by cloud microorganisms (Bianco et al., 2019). Thus, microbial processes in cloud water may

represent efficient sinks for numerous organics and might even result in products different from those of chemical reactions (Husárová et al., 2011). Thus, atmospheric models may be incomplete in describing the loss of some organic compounds and should be complemented by microbial processes in order to give a complete representation of the atmospheric multiphase system. While it has been recognized for a long time that microbial remediation in the environment is a common process (Kumar et al., 2011; Watanabe, 2001), we suggest that the atmosphere represents an additional medium for such processes.

## 5. Summary and conclusions

The newly derived biodegradation data for *Rhodococcus* with phenol and catechol were implemented in a multiphase box model, together with additional literature data for *Pseudomonas* degradation of the two aromatics and their chemical radical processes in the gas and aqueous phases. Model results reveal for the chosen model conditions ($[^{\bullet}OH]_{gas}$ = $5 \cdot 10^{6}$ $cm^{-3}$; $[NO_3^{\bullet}]_{gas}$ = $5 \cdot 10^{8}$ $cm^{-3}$; $[^{\bullet}OH]_{aq} \sim 10^{-15}$ M; $[NO_3^{\bullet}]_{aq} \sim 10^{-14}$ M; [Bacteria cell] =$1.7 \cdot 10^{7}$ cell $mL^{-1}$), the chemical and microbial activities in the aqueous phase are comparable. However, for catechol the loss processes in the aqueous phase are relatively more important (~30% of total loss) than for phenol (0.1% of total loss) due to its much greater water solubility ($K_{H,Phenol}$ = 647 M $atm^{-1}$; $K_{H,catechol}$ = $8.3 \cdot 10^{5}$ M $atm^{-1}$). It can be concluded that under some atmospheric conditions, the loss of highly soluble organics may be underestimated by chemical reactions only as the biodegradation of these organics by bacteria (and possibly other microorganisms) could represent additional sinks resulting in different products. Our model approach is highly simplified and limited in terms of biological, chemical and cloud microphysical conditions. More comprehensive experimental and model studies are needed to explore parameters spaces for relevant cloud water constituents (highly water-soluble, relatively low chemical reactivity) in order to better quantify the role of bacteria and other microorganisms in clouds as active entities that take part in the conversion of organics in the atmospheric multiphase system.

**Data availability:** All experimental and additional model data can be obtained from the authors upon request.

**Author contributions:** AMD and GM designed the experiments in microcosms. SJ, AL, MS and ML performed the experiments. BE performed the model simulations. BE and AMD wrote the manuscript.

**Competing interests**: The authors declare that they have no conflict of interest.

**Acknowledgements:** This work was funded by the French National Research Agency (ANR) in the framework of the 'Investment for the Future' program, ANR-17-MPGA-0013. S. Jaber is recipient of a school grant from the Walid Joumblatt Foundation for University Studies (WJF), Beirut, Lebanon and A. Lallement from the BIOCLOUD ANR project (N° ANR-13-BS06-004-01).

## References


Al-Khalid, T. and El-Naas, M. H.: Aerobic Biodegradation of Phenols: A Comprehensive Review, Crit. Rev. Environ. Sci. Technol., 42(16), 1631–1690, doi:10.1080/10643389.2011.569872, 2012.

Amato, P., Joly, M., Besaury, L., Oudart, A., Taib, N., Moné, A. I., Deguillaume, L., Delort, A. and Debroas, D.: Active microorganisms thrive among extremely diverse communities in cloud water, PLOS One, 12(8), doi:doi.org/10.1371/journal.pone.0182869, 2017.

Amato, P., Besaury, L., Joly, M., Penaud, B., Deguillaume, L. and Delort, A.-M.: Metatranscriptomic exploration of microbial functioning in clouds, Sci. Rep., 9(1), 4383, doi:10.1038/s41598-019-41032-4, 2019.

Arakaki, T., Anastasio, C., Kuroki, Y., Nakajima, H., Okada, K., Kotani, Y., Handa, D., Azechi, S., Kimura, T., Tsuhako, A. and Miyagi, Y.: A general scavenging rate constant for reaction of hydroxyl radical with organic carbon in atmospheric waters, Env. Sci Technol, 47(15), 8196–8203, doi:10.1021/es401927b, 2013.

Ariya, P. A., Nepotchatykh, O., Ignatova, O. and Amyot, M.: Microbiological degradation of atmospheric organic compounds, Geophys. Res. Lett., 29(22), doi: 10.1029/2002GL015637, 2002.

Bahadur, R., Uplinger, T., Russell, L. M., Sive, B. C., Cliff, S. S., Millet, D. B., Goldstein, A. and Bates, T. S.: Phenol Groups in Northeastern U.S. Submicrometer Aerosol Particles Produced from Seawater Sources, Environ. Sci. Technol., 44(7), 2542–2548, doi:10.1021/es9032277, 2010.

Beales, N.: Adaptation of Microorganisms to Cold Temperatures, Weak Acid Preservatives, Low pH, and Osmotic Stress: A Review, Compr. Rev. Food Sci. Food Saf., 3(1), 1–20, doi:10.1111/j.1541-4337.2004.tb00057.x, 2004.

Bianco, A., Deguillaume, L., Chaumerliac, N., Vaïtilingom, M., Wang, M., Delort, A.-M. and Bridoux, M. C.: Effect of endogenous microbiota on the molecular composition of cloud water: a study by Fourier-transform ion cyclotron resonance mass spectrometry (FT-ICR MS), Sci. Rep., 9(1), 7663, doi:10.1038/s41598-019-44149-8, 2019.

Bolzacchini, E., Bruschi, M., Hjorth, J., Meinardi, S., Orlandi, M., Rindone, B. and Rosenbohm, E.: Gas-Phase Reaction of Phenol with NO3, Environ. Sci. Technol., 35(9), 1791–1797, doi:10.1021/es001290m, 2001.

Brigante, M. and Mailhot, G.: Chapter 9: Phototransformation of Organic Compounds Induced by Iron Species, in Surface Water Photochemistry, pp. 167–195., 2015.

Chow, K. S., Huang, X. H. H. and Yu, J. Z.: Quantification of nitroaromatic compounds in atmospheric fine particulate matter in Hong Kong over 3 years: field measurement evidence for secondary formation derived from biomass burning emissions, Environ. Chem., 13(4), 665–673, 2016.

Deguillaume, L., Charbouillot, T., Joly, M., Vaïtilingom, M., Parazols, M., Marinoni, A., Amato, P., Delort, A. M., Vinatier, V., Flossmann, A., Chaumerliac, N., Pichon, J. M., Houdier, S., Laj, P., Sellegri, K., Colomb, A., Brigante, M. and Mailhot, G.: Classification of clouds

sampled at the puy de Dôme (France) based on 10 yr of monitoring of their physicochemical properties, Atmos Chem Phys, 14(3), 1485–1506, doi:10.5194/acp-14-1485-2014, 2014.

Delhomme, O., Morville, S. and Millet, M.: Seasonal and diurnal variations of atmospheric concentrations of phenols and nitrophenols measured in the Strasbourg area, France, Atmospheric Pollut. Res., 1(1), 16–22, doi:10.5094/APR.2010.003, 2010.

Delort, A.-M., Vaïtilingom, M., Amato, P., Sancelme, M., Parazols, M., Mailhot, G., Laj, P. and Deguillaume, L.: A short overview of the microbial population in clouds: Potential roles in atmospheric chemistry and nucleation processes, Atmos Res, 98(2–4), 249–260, doi:10.1016/j.atmosres.2010.07.004, 2010.

Ervens, B., George, C., Williams, J. E., Buxton, G. V., Salmon, G. A., Bydder, M., Wilkinson, F., Dentener, F., Mirabel, P., Wolke, R. and Herrmann, H.: CAPRAM2.4 (MODAC mechanism): An extended and condensed tropospheric aqueous phase mechanism and its application, J Geophys Res, 108(D14), 4426, doi:doi: 10.1029/2002JD002202, 2003.

Ervens, B., Sorooshian, A., Lim, Y. B. and Turpin, B. J.: Key parameters controlling OH-initiated formation of secondary organic aerosol in the aqueous phase (aqSOA), J Geophys Res - Atmos, 119(7), 3997–4016, doi:10.1002/2013JD021021, 2014.

Fankhauser, A. M., Antonio, D. D., Krell, A., Alston, S. J., Banta, S. and McNeill, V. F.: Constraining the Impact of Bacteria on the Aqueous Atmospheric Chemistry of Small Organic Compounds, ACS Earth Space Chem., 3(8), 1485–1491, doi:10.1021/acsearthspacechem.9b00054, 2019.

Guan, N. and Liu, L.: Microbial response to acid stress: mechanisms and applications, Appl. Microbiol. Biotechnol., 104(1), 51–65, doi:10.1007/s00253-019-10226-1, 2020.

Gurol, M. D. and Nekouinaini, S.: Kinetic behavior of ozone in aqueous solutions of substituted phenols, Ind. Eng. Chem. Fundam., 23(1), 54–60, doi:10.1021/i100013a011, 1984.

Harrison, M. A. J., S. Barra, D. Borghesi, D. Vione, C. Arsene and R. I. Olariu: Nitrated phenols in the atmosphere: A review, Atmos Env., 39, 231–248, 2005.

Herrmann, H., Ervens, B., Jacobi, H.-W., Wolke, R., Nowacki, P. and Zellner, R.: CAPRAM2.3: A Chemical Aqueous Phase Radical Mechanism for Tropospheric Chemistry, J Atmos Chem, 36, 231–284, 2000.

Hinteregger, C., Leitner, R., Loidl, M., Ferschl, A. and Streichsbier, F.: Degradation of phenol and phenolic compounds by Pseudomonas putida EKII, Appl. Microbiol. Biotechnol., 37(2), 252–259, doi:10.1007/BF00178180, 1992.

Hoffmann, E. H., Tilgner, A., Wolke, R., BÃ¶ge, O., Walter, A. and Herrmann, H.: Oxidation of substituted aromatic hydrocarbons in the tropospheric aqueous phase: kinetic mechanism development and modelling, Phys. Chem. Chem. Phys., 20(16), 10960–10977, doi:10.1039/C7CP08576A, 2018.

Hsieh, C.-C., Chang, K.-H. and Kao, Y.-S.: Estimating the ozone formation potential of volatile aromatic compounds in vehicle tunnels, Chemosphere, 39(9), 1433–1444, doi:10.1016/S0045-6535(99)00045-4, 1999.

Husárová, S., Vaïtilingom, M., Deguillaume, L., Traikia, M., Vinatier, V., Sancelme, M., Amato, P., Matulová, M. and Delort, A.-M.: Biotransformation of methanol and formaldehyde by bacteria isolated from clouds. Comparison with radical chemistry, Atmos. Environ., 45(33), 6093–6102, doi:https://doi.org/10.1016/j.atmosenv.2011.06.035, 2011.

Kumar, A., Bisht, B. S., Joshi, V. D. and Dhewa, T.: Review on Bioremediation of Polluted Environment: A Management Tool, Int. J. Environ. Sci., 1(6), 1079–1093, doi:10.1.1.422.2461-3, 2011.

Lallement, A., Besaury, L., Eyheraguibel, B., Amato, P., Sancelme, M., Mailhot, G. and Delort, A. M.: Draft Genome Sequence of Rhodococcus enclensis 23b-28, a Model Strain Isolated from Cloud Water, Genome Announc., 5(43), e01199-17, doi:10.1128/genomeA.01199-17, 2017.

Lallement, A., Vinatier, V., Brigante, M., Deguillaume, L., Delort, A. M. and Mailhot, G.: First evaluation of the effect of microorganisms on steady state hydroxyl radical concentrations in atmospheric waters, Chemosphere, 212, 715–722, doi:10.1016/j.chemosphere.2018.08.128, 2018a.

Lallement, A., Besaury, L., Tixier, E., Sancelme, M., Amato, P., Vinatier, V., Canet, I., Polyakova, O. V., Artaev, V. B., Lebedev, A. T., Deguillaume, L., Mailhot, G. and Delort, A.-M.: Potential for phenol biodegradation in cloud waters, Biogeosciences, 15(18), 5733–5744, doi:10.5194/bg-15-5733-2018, 2018b.

Lebedev, A. T., Polyakova, O. V., Mazur, D. M., Artaev, V. B., Canet, I., Lallement, A., Vaïtilingom, M., Deguillaume, L. and Delort, A.-M.: Detection of semi-volatile compounds in cloud waters by GC×GC-TOF-MS. Evidence of phenols and phthalates as priority pollutants, Environ. Pollut., 241, 616–625, doi:10.1016/j.envpol.2018.05.089, 2018.

Levsen, K., Behnert, S., Mußmann, P., Raabe, M. and Prieß, B.: Organic Compounds In Cloud And Rain Water, Int. J. Environ. Anal. Chem., 52(1–4), 87–97, doi:10.1080/03067319308042851, 1993.

Li, J., Mailhot, G., Wu, F. and Deng, N.: Photochemical efficiency of Fe(III)-EDDS complex: OH radical production and 17β-estradiol degradation, J. Photochem. Photobiol. Chem., 212(1), 1–7, doi:10.1016/j.jphotochem.2010.03.001, 2010.

Lüttke, J. and Levsen, K.: Phase partitioning of phenol and nitrophenols in clouds, Gt. Dun Fell Cloud Exp. 1993 Eurotrac Sub-Proj. Ground-Based Cloud Exp. GCE, 31(16), 2649–2655, doi:10.1016/S1352-2310(96)00228-2, 1997.

Lüttke, J., Scheer, V., Levsen, K., Wünsch, G., Neil Cape, J., Hargreaves, K. J., Storeton-West, R. L., Acker, K., Wieprecht, W. and Jones, B.: Occurrence and formation of nitrated phenols in and out of cloud, Gt. Dun Fell Cloud Exp. 1993 Eurotrac Sub-Proj. Ground-Based Cloud Exp. GCE, 31(16), 2637–2648, doi:10.1016/S1352-2310(96)00229-4, 1997.

Ng, N. L. ;, Kroll, J. H., Chan, A. W. H., Chhabra, P. S., Flagan, R. C. and Seinfeld, J. H.: Secondary organic aerosol formation from m-xylene, toluene, and benzene, Atmos Chem Phys, 7, 3909–3922, 2007.

Pillar, E. A., Camm, R. C. and Guzman, M. I.: Catechol Oxidation by Ozone and Hydroxyl Radicals at the Air–Water Interface, Environ. Sci. Technol., 48(24), 14352–14360, doi:10.1021/es504094x, 2014.

Razika, B., Abbes, C., Messaoud, C. and Soufi, K.: Phenol and Benzoic Acid Degradation by Pseudomonas aeruginosa, J. Water Resour. Prot., 2(9), 788–791, 2010a.

Razika, B., Abbes, B., Messaoud, C. and Soufi, K.: Phenol and Benzoic Acid Degradation by Pseudomonas aeruginosa, J. Water Resour. Prot., 788–791, 2010b.

Reasoner, D. J. and Geldreich, E. E.: A new medium for the enumeration and subculture of bacteria from potable water, Appl. Environ. Microbiol., 49(1), 1–7, 1985.

Schwartz, S.: Mass transport considerations pertinent to aqueous phase reactions of gases in liquid water clouds, in Chemistry of Multiphase Atmospheric Systems, vol. 6, edited by W. Jaeschke, pp. 415–471, Springer, Berlin., 1986.

Straube, G.: Phenol hydroxylase from Rhodococcus sp. P 1, J. Basic Microbiol., 27(4), 229–232, doi:10.1002/jobm.3620270415, 1987.

TOXNET Toxicology Data Network: TOXNET, Toxicol. Data Netw. [online] Available from: https://toxnet.nlm.nih.gov/ newtoxnet/hsdb.htm (Accessed 6 November 2019), 2019.

Vaïtilingom, M.: Atmospheric chemistry of carboxylic acids: microbial implication versus photochemistry, Atmos Chem Phys, 11, doi:10.5194/acp-11-8721-2011, 2011.

Vaïtilingom, M., Amato, P., Sancelme, M., Laj, P., Leriche, M. and Delort, A.-M.: Contribution of Microbial Activity to Carbon Chemistry in Clouds, Appl. Environ. Microbiol., 76(1), 23–29, doi:10.1128/AEM.01127-09, 2010.

Vaïtilingom, M., Charbouillot, T., Deguillaume, L., Maisonobe, R., Parazols, M., Amato, P., Sancelme, M. and Delort, A. M.: Atmospheric chemistry of carboxylic acids: microbial implication versus photochemistry, Atmos Chem Phys, 11(16), 8721–8733, doi:10.5194/acp-11-8721-2011, 2011.

Vaïtilingom, M., Attard, E., Gaiani, N., Sancelme, M., Deguillaume, L., Flossmann, A. I., Amato, P. and Delort, A.-M.: Long-term features of cloud microbiology at the puy de Dôme (France), Atmos. Environ., 56(0), 88–100, doi:http://dx.doi.org/10.1016/j.atmosenv.2012.03.072, 2012.

Vaïtilingom, M., Deguillaume, L., Vinatier, V., Sancelme, M., Amato, P., Chaumerliac, N. and Delort, A.-M.: Potential impact of microbial activity on the oxidant capacity and organic carbon budget in clouds, Proc. Natl. Acad. Sci., 110(2), 559–564, doi:10.1073/pnas.1205743110, 2013.

Vinatier, V., Wirgot, N., Joly, M., Sancelme, M., Abrantes, M., Deguillaume, L. and Delort, A.-M.: Siderophores in Cloud Waters and Potential Impact on Atmospheric Chemistry: Production by Microorganisms Isolated at the Puy de Dôme Station, Environ. Sci. Technol., 50(17), 9315–9323, doi:10.1021/acs.est.6b02335, 2016.

Vione, D., Maurino, V., Minero, C., Vincenti, M. and Pelizzetti, E.: Aromatic photonitration in homogeneous and heterogeneous aqueous systems, Environ. Sci. Pollut. Res., 10(5), 321–324, doi:10.1065/espr2001.12.104.1, 2003.

Watanabe, K.: Microorganisms relevant to bioremediation, Curr. Opin. Biotechnol., 12(3), 237–241, doi:10.1016/S0958-1669(00)00205-6, 2001.

Xie, M., Chen, X., Hays, M. D., Lewandowski, M., Offenberg, J., Kleindienst, T. E. and Holder, A. L.: Light Absorption of Secondary Organic Aerosol: Composition and Contribution of Nitroaromatic Compounds, Environ. Sci. Technol., 51(20), 11607–11616, doi:10.1021/acs.est.7b03263, 2017.

Xu, C. and Wang, L.: Atmospheric Oxidation Mechanism of Phenol Initiated by OH Radical, J. Phys. Chem. A, 117(11), 2358–2364, doi:10.1021/jp308856b, 2013.

Yu, L., Smith, J., Laskin, A., Anastasio, C., Laskin, J. and Zhang, Q.: Chemical characterization of SOA formed from aqueous-phase reactions of phenols with the triplet excited state of carbonyl and hydroxyl radical, Atmos Chem Phys, 14(24), 13801–13816, doi:10.5194/acp-14-13801-2014, 2014.

# Supporting information

# Biodegradation of phenol and catechol in cloud water: Comparison to chemical oxidation in the atmospheric multiphase system

Saly Jaber[1], Audrey Lallement[1], Martine Sancelme[1], Martin Leremboure[1], Gilles Mailhot[1], Barbara Ervens[1*] and Anne-Marie Delort[1*]

[1]Université Clermont Auvergne, CNRS, SIGMA Clermont, Institut de Chimie de Clermont-Ferrand, F-63000 Clermont-Ferrand, France

*Correspondence to:* Anne-Marie Delort (a-marie.delort@uca.fr) and Barbara Ervens (barbara.ervens@uca.fr)

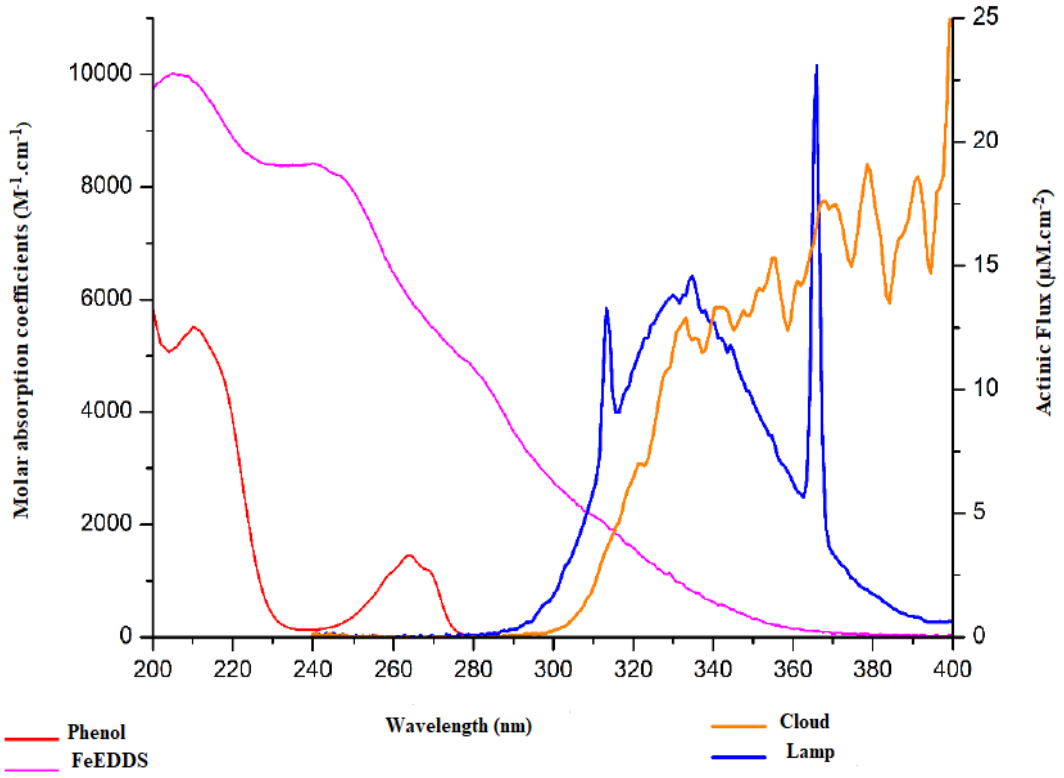


***Figure S- 1 :*** *Comparison of the actinic fluxes of the lamps used and the emission of the solar spectrum measured in-cloud at the puy de Dôme station. The blue line represents the actinic flux of the lamp; the brown line corresponds to the actinic flux of the solar emission spectrum in cloud. The pink line represents the molar absorption coefficient of the Fe-EDDS complex. The red line represents the molar absorption coefficient of phenol.*

## Section S-1 Calculation of the biodegradation rates for the *Pseudomonas* strains

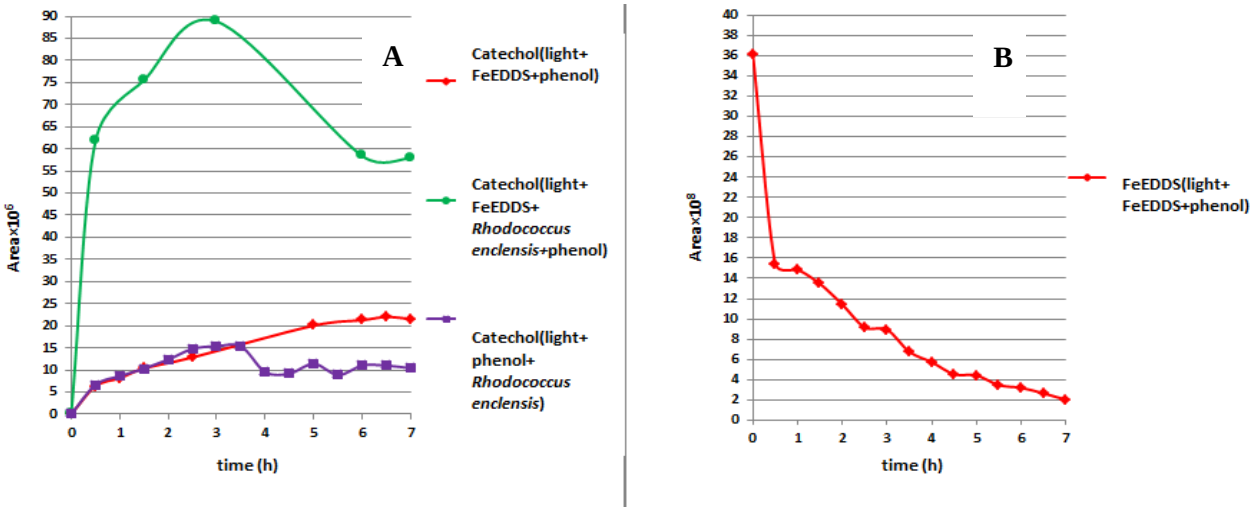


***Figure S- 2 :*** *A) time dependence of the integral of catechol signal (m/z= 110.03678) detected in mass spectra of incubations with Fe(EDDS)+light and Phenol (red), Fe(EDDS)+ light, Phenol and R. enclensis (green), light + Phenol and* R. enclensis *without Fe(EDDS)(violet). B) Time dependence of the integral of Fe(EDDS) signal (m/z = 346.0086) detected in the mass spectrum, recorded during the incubation with Fe(EDDS)+ light and Phenol.*

### *S-1.1 Pseudomonas putida* EKII

To calculate the biodegradation rate of phenol and catechol by *Pseudomonas putida* EKII, based on experiments performed at pH = 7.0, we used the following data from Hinteregger et al. (1992):

**Phenol:** Biodegradation of 654 μmol $L^{-1}$ $h^{-1}$, number of cells: 3.3 ·$10^9$ cell $L^{-1}$

**Biodegradation rate of phenol: 1.98·$10^{-17}$ mol $cell^{-1}$ $h^{-1}$**

**Catechol:** Biodegradation rate of catechol is twelve times higher than of phenol (ratio = 2.4μmol $min^{-1}$ $mg^{-1}$ / 0.2 μmol $min^{-1}$ $mg^{-1}$, expressed per mg of cells)

**Biodegradation of catechol: 1.98·$10^{-17}$ ·12 = 23.78 ·$10^{-17}$ mol $cell^{-1}$ $h^{-1}$**

### *S-1.2 Pseudomonas aeruginosa*

To calculate the biodegradation rate of phenol and catechol by *Pseusomonas aeriginosa*, based on experiments performed at pH=7.0, we used the following data from Razika et al. (2010):

**Phenol:** Biodegradation of 10 mg $L^{-1}$ during 96 hours, number concentration of cells: 4.7. $10^9$ cell $L^{-1}$

**Biodegradation rate of phenol: 23.49·$10^{-17}$ mol $cell^{-1}$ $h^{-1}$**

Biodegradation of 50 mg $L^{-1}$ during 120 hours, number concentration of cells: 4.7·$10^9$ cell $L^{-1}$

**Biodegradation rate of phenol: 94.31·$10^{-17}$ mol $cell^{-1}$ $h^{-1}$**

**Biodegradation rate of phenol (average value) taken into account: 58.9·$10^{-17}$ mol $cell^{-1}$ $h^{-1}$**

**Catechol:** No information is available in Razika et al (2010), so we multiplied the biodegradation rates of phenol with a factor of twelve as it is within the same order of magnitude of what we found in our study (Factor ~ 10)

**Biodegradation rate of catechol (average value): 58.9·$10^{-17}$ mol $cell^{-1}$ $h^{-1}$·12= 706.8 $10^{-17}$ mol $cell^{-1}$.**

## Section S-2: Calculation of photolysis rate j(Fe(EDDS)) and resulting OH concentration in the experiments

$$j = \int_{250}^{400} I_{0,\lambda} \cdot \varepsilon_\lambda \cdot \phi_\lambda \cdot d\lambda \; \frac{photons}{cm^2\ s\ nm} \frac{cm^3}{molec\ cm} \frac{nm}{} \qquad [s^{-1}]$$

$I_{0,\lambda}$ = spectral actinic flux [photons $cm^{-2}$ $s^{-1}$ $nm^{-1}$]

$\varepsilon_\lambda$ = extinction coefficient [$cm^3$ $molec^{-1}$ $cm^{-1}$]

$\phi_\lambda$ = Quantum yield [dimension less]

---

**Experimental data**

Irradiance E(λ) [μW $cm^{-2}$] ; convert into SI units  E'[$W/m^2$] = E·$10^{-6}$ W/μW ·$10^4$ $cm^2/m^2$ = E·0.01

Convert irradiance E(λ) [μW $cm^{-2}$] to actinic flux I [photons $cm^{-2}$ $s^{-1}$]:

Actinic flux $I' = \frac{E\prime\,\lambda}{h \cdot c} \left[\frac{W\ m}{m^2} \frac{s}{J\ s\ m}\right] = \frac{E\,\lambda}{h \cdot c} \left[\frac{kg\ m^2}{s^3 m^2} \frac{m}{} \frac{s^2}{kg\ m^2 s} \frac{s}{m}\right] = \frac{photons}{m^2\ s}$

Spectral actinic flux $I_\lambda = \frac{I'}{\lambda} \cdot\ 10^{-4} = \frac{E(\lambda)}{h \cdot c} \left[\frac{W}{m^2} \frac{s}{J\ s\ m}\right] = \frac{E\,\lambda}{h \cdot c} \left[\frac{kg\ m^2}{s^3 m^2} \frac{m}{} \frac{s^2}{kg\ m^2 s} \frac{s}{m}\right] = \frac{photons}{cm^2\ s\ nm}$

h = 6.62606×$10^{-34}$ J s

c = 3·$10^8$ m/s

ε'  molar absorption coefficient (L $mol^{-1}$ $cm^{-1}$)  = extinction coefficient

$\varepsilon_\lambda$ = ε' $\frac{L}{mol\ cm} \cdot \frac{1000\ cm^3}{L} \cdot \frac{mol}{6.022e23\ molec} = \varepsilon' \cdot 1000/N_A$ [$cm^3$ $molec^{-1}$ $cm^{-1}$]

---

Quantum yield: $\phi_\lambda$ = 0.025 (at 290 < λ < 400 nm)

$$j = \int_{250}^{400} I_\lambda \cdot \varepsilon_\lambda \cdot \phi_\lambda \cdot d\lambda \; \frac{photons}{cm^2\ s\ nm} \frac{cm^3}{molec\ cm} \frac{nm}{} = \mathbf{0.001388\ s^{-1}}$$

---

**Calculation of steady-state References: •OH(aq) concentration**

<u>OH formation:</u>

[Fe-EDDS] + hν → •OH + products  j = 1.388e-3 $s^{-1}$  $[Fe(EDDS)]_0$ = 0.5 mM

$$-\frac{d[Fe(EDDS)]}{dt} = \frac{d[OH]}{dt} = j\,[Fe(EDDS)]$$

<u>•OH loss</u>

•OH + Phenol → Products  k = 8.41e9 $M^{-1}$ $s^{-1}$  $[Phenol]_0$ = 0.1 mM

$$\frac{d[OH]}{dt} = -\,k\,[OH][Phenol]$$

→ Steady-state OH concentration at the beginning of experiment

k [•OH] [Phenol] = j [Fe(EDDS)]

$$[OH] = \frac{j\,[Fe(EDDS)]}{k\,[Phenol]} = \frac{1.388e-3\ s^{-1}\ 5e-4\ M}{8.41e9\ M^{-1}s^{-1}\ \ 1e-4\ M} = 8.3e-13\ M$$

## Section S-3: Input data to the multiphase box model

### S-3.1: Multiphase processes

***Table S-1:*** *Chemical and microbial processes in the multiphase model*

| **Gas Phase** | | |
|---|---|---|
| | **Chemical rate constant [$cm^3$ $s^{-1}$]** | **Reference** |
| $^{\bullet}OH$ + Phenol → 0.5 Catechol + 0.5 Prod [a)] | $2.81 \cdot 10^{-11}$ | (Berndt and Böge, 2001) |
| $NO_3^{\bullet}$ + Phenol → Products | $5.8 \cdot 10^{-12}$ | (Bolzacchini et al., 2001) |
| $^{\bullet}OH$ + Catechol → Products | $1.1 \cdot 10^{-10}$ | (Olariu et al., 2000) |
| $NO_3^{\bullet}$ + Catechol → Products | $9.8 \cdot 10^{-11}$ | (Olariu et al., 2004) |
| **Aqueous phase** | | |
| | **Chemical rate constant [$M^{-1}$ $s^{-1}$]** | |
| $^{\bullet}OH$ + Phenol → 0.5 Catechol + 0.5 Prod [b)] | $8.41 \cdot 10^{9}$ | (Raghavan and Steenken, 1980) |
| $NO_3^{\bullet}$ + Phenol → Products | $1.9 \cdot 10^{9}$ | (Umschlag et al., 2002) |
| $^{\bullet}OH$ + Catechol → Products | $4.7 \cdot 10^{9}$ | (Hoffmann et al., 2018) |
| $NO_3^{\bullet}$ + Catechol → Products | $1.9 \cdot 10^{9}$ | (Hoffmann et al., 2018) |
| $^{\bullet}OH$ + WSOC → Products | $2 \cdot 10^{6}$ $s^{-1}$ | Based on (Arakaki et al., 2013), assuming [WSOC] = 5 mM |
| $NO_3$ → Products | $10^{5}$ $s^{-1}$ | Based on (Exner et al., 1992; Zellner and Herrmann, 1994); assuming 1 mM $Cl^-$, 0.01 mM $Br^-$ |
| The following three reactions are only considered in sensitivity simulations, Figure S-4 | | |
| $O_3$ + Phenol → Products | 1300 | (Hoigné and Bader, 1983) |
| $O_3$ + Catechol → Products | $3.1 \cdot 10^{5}$ | (Gurol and Nekouinaini, 1984) |
| $HO_2^{\bullet}/O_2^{\bullet-}$ + Catechol → Products | $7.8 \cdot 10^{4}$ | Rate constant for $HO_2/O_2^-$ ratio at pH = 4 ($pK_a(HO_2^{\bullet})$ = 4.8) calculated based on $k_{HO2}$, $k_{O2}$- by (Bielski et al., 1985) |

| | **Microbial rate constant [L $cell^{-1}$ $s^{-1}$]** | |
|---|---|---|
| *Rhodococcus* + Phenol → Catechol | $1.8 \cdot 10^{-13}$ | [d)] |
| *Rhodococcus* + Catechol → Products | $1.5 \cdot 10^{-12}$ | [d)] |
| *Pseudomonas* + Phenol → Catechol | $1 \cdot 10^{-13}$ | [d)] |
| *Pseudomonas* + Catechol → Prod | $1.2 \cdot 10^{-12}$ | [d)] |

| **Phase transfer processes** | | | | |
|---|---|---|---|---|
| | **$K_H$ [M $atm^{-1}$]** | **Reference** | **$\alpha$ [c)]** | **$D_g$ [$cm^2$ $s^{-1}$][c)]** |
| $^{\bullet}OH(aq) \leftrightarrow {}^{\bullet}OH(gas)$ | 25 | (Kläning et al., 1985) | 0.05 | 0.15 |
| $NO_3^{\bullet}(aq) \leftrightarrow NO_3^{\bullet}(gas)$ | 0.6 | (Rudich et al., 1996) | 0.1 | 0.1 |
| Phenol(aq) ↔ Phenol(gas) | 647 | (Feigenbrugel et al., 2004) | 0.027 | 0.09 |
| Catechol(aq) ↔ Catechol(gas) | $8.31 \cdot 10^{5}$ | (Sander, 2015) | 0.1 | 0.08 |

[a)] Catechol yield likely represents an upper estimate for the total of all dihydroxybenzene compounds [b)] Initial formation of the phenoxy radical and the subsequent reaction with $O_2$ are lumped here, leading to 0.5 catechol into one step since the second reaction is diffusion controlled; [c)] These values were taken from CAPRAM (Ervens et al., 2003; Hoffmann et al., 2018) [d)] See calculation of values in Section S-3.2

### S-3.2 Calculation of microbial rate constants from experimentally derived rates

Experimentally-derived rates R of microbial activity towards phenol and catechol are summarized in Table 2 of the main part of the manuscript, together with the bacteria type (*Rhodococcus*, *Pseudomonas putida*, *Pseudomonas aeruginosa*) and aqueous phase concentrations of substrate (phenol, catechol) and bacteria cells. Strictly, the measured rates might be only valid for the same substrate-to-cell ratio as the substrate availability determines the cell activity. Since these concentrations differ greatly, we derive the first-order rate constant k' [$h^{-1}$]

$$k' = R\,[Cell] / [Substrate] \quad \text{(S-1)}$$

Ambient cell concentrations in cloud water are on the order of $10^6 – 10^8$ cell $L^{-1}$. We assume a total cell concentration of $6.8 \cdot 10^7$ cell $L^{-1}$ of which 3.6% are *Rhodococcus* ($C_{Rh,cloud} = 2.7 \cdot 10^6$ cell $L^{-1}$) and 19.5% *Pseudomonas* ($C_{Ps,cloud} = 1.3 \cdot 10^7$ cell $L^{-1}$). Phenol concentrations in cloud water are in the range of 5.5 - 7.7 nM (Lebedev et al., 2018). Using the lower value of this range yields phenol-to-cell ratios in cloud water of $2 \cdot 10^{-15}$ mol $cell^{-1}$ and $4.2 \cdot 10^{-16}$ mol $cell^{-1}$ for *Rhodococcus* and *Pseudomonas*, respectively, which is within two orders of magnitude of the ratios as used in the experiments. Corresponding cloud water measurements for catechol are not available.

In the multiphase model, we describe the microbial processes analogous to chemical reactions, i.e. with a formal second-order rate constant in units of L $cell^{-1}$ $s^{-1}$ using the constant cell concentrations in the aqueous phase.

$$k_{2nd}\,[L\ cell^{-1}\ s^{-1}] = k' \ / \ [Cell]_{cloud} \ / 3600\ s\ h^{-1} \quad \text{(S-2)}$$

The resulting $k_{2nd}$ are then used in the model studies for the assumed (constant) cell concentrations in cloud water.

### S 3.3 Considerations of potential pH dependence of the chemical and biodegradation rates

It can be expected that none of the rates in Eq-2 shows any significant dependence on cloud relevant pH values due to the following reasoning:

$k_{chem,gas}$: The gas phase rate constants describe chemical processes in the gas phase and, thus, are intendent of any solution properties, such as pH.

$k_{chem,aq}$: The rate constants of $NO_3$ and OH reactions with the phenolic aromatics are not expected to show any pH dependence since the reactions occur via H-abstraction and thus the rate constants are a function of the bond strength of the hydrogen bonds (e.g. discussion in (Herrmann, 2003)). Even though the rate constant of NO3 and OH with phenol and catechol have not been investigated as a function of pH, the small variability of rate constants of other alcohols (e.g. NIST solution data base), suggests that our assumption of a pH-independent $k_{chem,aq}$ is reasonable. Only if the pH value increases to very high pH values, i.e. near the acid dissociation values of phenols ($pK_a \sim 10$), differences in the reaction mechanisms (e.g. electron transfer) and, thus, in rate constants may be expected.

$k_{bact,aq}$: We have shown in previous studies that the biodegradation rates for several organics and bacteria strains do not show any systematic dependence on pH within a range of ~5 < pH < ~6.3 (Vaïtilingom et al., 2011). This insensitivity to the surrounding solution pH is expected: Unlike chemical reactions, the biodegradation does not occur in the surrounding water phase, but within the bacteria cells which self-regulate their pH values to a range of 6.5-7, even if the surrounding pH varies over wide ranges. Only at very acidic (pH < 2) or very alkaline (pH > 10) solutions, the internally buffered pH value within the cells might be different.

[Radical]: For both radicals, OH and $NO_3$, the main source in the aqueous phase is the direct uptake from the gas phase, e.g. (Ervens et al., 2003; Tilgner et al., 2013). Since gas phase processes are independent of pH, the radical gas phase concentration is not affected by the solution pH. Other source processes of the OH(aq) radical include aqueous phase reactions, such as the direct photolysis of $H_2O_2$ or Fenton reactions (reactions of iron(II) with hydroperoxides), which also do not show any pH dependence over the range of relevant values (~2< pH < ~7)

**[Aromatic]:** The concentrations of the aromatics are initial values of the model. Given that [Aromatic] is included in all three terms in Eq-R1, they cancel anyway in the comparison of the three terms for a given simulation.

**$K_H$:** Henry's laws constants for the radicals or aromatics, respectively, do not show any pH dependence. Admittedly, there are only very few pH dependent measurements available for these and related compounds. However, since Henry's law

Only at very high pH values, i.e. near the pKa values of the phenols (pH ~ 10), the effective Henry's law constants for the aromatics maybe higher than the physical Henry's law constants. As pH value of cloud water is significantly below this threshold, it is safe to neglect this dissociation.

α: The mass accommodation coefficient describes the probability of a molecule to 'stick' on a surface upon collision. There is no physical reason why this process should pH dependent and no data that corroborate such a dependency.

$D_g$: Gas phase diffusion is a process that occurs only in the gas phase and thus is independent of any solution properties (including pH).

***Table S-2:*** *Summary of literature data on microbial activity towards phenol and catechol by Rhodococcus and Pseudomonas. For the estimates of unknown rates, refer to Section 3.2 (Comparison to literature data) in the main part of the manuscript*

| **Substrate** | **Bacteria type** | **R** / **mol cell$^{-1}$ h$^{-1}$** | **[Substrate]** / **M** | **[Cell]$_{experiment}$** / **(cell L$^{-1}$)** | **Ref** | **[Substrate]/ [Cell]** / **mol cell$^{-1}$** | **k'** / **h$^{-1}$** | **[Cell]$_{cloud}$** | **k$_{2nd}$** / **L cell$^{-1}$ s$^{-1}$** |
|---|---|---|---|---|---|---|---|---|---|
| Phenol | *Rhodococcus* | $1.76\cdot10^{-16}$ | $10^{-4}$ | $10^{9}$ | a | $10^{-13}$ | $1.76\cdot10^{-3}$ | $2.7\cdot10^{6}$ | $1.8\cdot10^{-13}$ |
| Catechol | *Rhodococcus* | $1.5\cdot10^{-15}$ | $10^{-4}$ | $10^{9}$ | b | $10^{-13}$ | $1.5\cdot10^{-2}$ | $2.7\cdot10^{6}$ | $1.5\cdot10^{-12}$ |
| Phenol | *Pseudomonas putida* | $1.99\cdot10^{-17}$ | $6.54\cdot10^{-4}$ | $3.3\cdot10^{9}$ | c | $2\cdot10^{-13}$ | $1\cdot10^{-4}$ | | |
| Catechol | *Pseudomonas putida* | $2.39\cdot10^{-16}$ | | | c | | $2.4\cdot10^{-3}$ | | |
| Phenol | *Pseudomonas* | $2.35\cdot10^{-16}$ | $1.06\cdot10^{-4}$ | $4.7\cdot10^{9}$ | d | $2.3\cdot10^{-14}$ | $1\cdot10^{-2}$ | | |
| | *aeruginosa* | $9.43\cdot10^{-16}$ | $5.31\cdot10^{-4}$ | $4.7\cdot10^{9}$ | | $1.1\cdot10^{-13}$ | $8.3\cdot10^{-3}$ | | |
| Catechol | *Pseudomonas aeruginosa* | | | | e | | 0.11 | | |
| Phenol | *Pseudomonas (Average)* | | | | | | $5\cdot10^{-3}$ | $1.3\cdot10^{7}$ | $1\cdot10^{-13}$ |
| Catechol | *Pseudomonas (Average)* | | | | | | | $1.3\cdot10^{7}$ | $1.2\cdot10^{-12}$ |

[a)] (Lallement et al., 2018), [b)] This study, [c)] (Hinteregger et al., 1992) [d)] (Razika et al., 2010), [e)] Scaled up from data for phenol by reference [d)] using the same ratio of activities to phenol and catechol (12) as for the average value for *Pseudomonas putida*

## Section S-4: Model sensitivity study including the aqueous phase reactions of phenol with ozone and of catechol with ozone and $HO_2^•/O_2^{•-}$

In a recent model study by (Hoffmann et al., 2018), it was suggested that catechol (and other dihydroxybenzenes) are efficiently oxidized not only by $^•OH$ but also by ozone and the hydroperoxy ($HO_2^•/O_2^{•-}$) radical. Also the reaction of phenol with ozone was included in this model study. In that latter model study, a rate constant of $k(O_3 + Catechol) = 5.2 \cdot 10^5\ M^{-1}\ s^{-1}$ was estimated. This rate constant is similar to an experimentally-derived value of $k(O_3 + Catechol) = 3.1 \cdot 10^5\ M^{-1}\ s^{-1}$ (Gurol and Nekouinaini, 1984). This latter study was performed at very acidic conditions (pH = 1.5) and a strong pH dependence of the rate constant was pointed out leading to a decreasing rate constant with increasing pH and resulting in the predominance of the $^•OH$ reaction at atmospherically-relevant pH values (~5).

Since the exact pH dependence is not available, we show in the following model results from a sensitivity studies including the $HO_2^•$ and $O_3$ reactions in order to provide an upper estimate of their role in the multiphase system. Initial concentrations of 0.1 ppt $HO_2^•$ and 40 ppb ozone in the gas phase are assumed and held constant throughout the simulation. In agreement with the model results by Hoffmann et al. (2018), we find large contributions of the ozone reactions in the aqueous phase to the total loss. The relative contributions of the ozone (57 – 68%) and $HO_2^•/O_2^{•-}$ (16 – 19%) reactions with catechol predicted here are also similar as predicted in the previous model study.

### S-4.2 Model results

All model results [relative contribution to total loss [%]) are summarized in Table S-3. The upper part of the table contains results for the base simulations as shown in Figure 4 (microbial aqueous phase processes and $^•OH$ and $NO_3^•$ reactions in gas and aqueous phases); the bottom part of the table includes results for the sensitivity simulations that also include $HO_2^•$(aq) and $O_3$(aq) reactions (Figure S-3).

***Table S-3:*** *Model results of base case and sensitivity simulations: Relative contributions to total loss of phenol and catechol, respectively*

| | | $^•OH$(g) | $NO_3^•$(g) | $^•OH$(aq) | $NO_3^•$(aq) | $O_3$(aq) | $HO_2^•$(aq) | *Rhodo-coccus* | *Pseudo-monas* |
|---|---|---|---|---|---|---|---|---|---|
| **Base case** | | | | | | | | | |
| Day | Phenol | 99.8 | 0 | 0.22 | 0 | - | - | 0.01 | 0.006 |
| | Catechol | 69.3 | 0 | 14 | 0 | - | - | 9.3 | 7.4 |
| Night | Phenol | 0 | 99.8 | 0 | 0.18 | - | - | 0.0005 | 0.00027 |
| | Catechol | 0 | 97.5 | 0 | 2.2 | - | - | 0.18 | 0.14 |
| **Sensitivity simulation including aqueous phase reactions of $O_3$ (phenol, catechol) and $HO_2/O_2^-$ (catechol)** | | | | | | | | | |
| Day | Phenol | 99.7 | 0 | 0.22 | 0 | 0.02 | 0 | 0.01 | 0.0056 |
| | Catechol | 6.1 | 0 | 1.2 | 0 | 58.9 | 33 | 0.81 | 0.65 |
| Night | Phenol | 0 | 99.8 | 0 | 0.18 | 0.0007 | 0 | 0.0005 | 0.00027 |
| | Catechol | 0 | 86.4 | 0 | 2 | 11.4 | 0 | 0.16 | 0.13 |

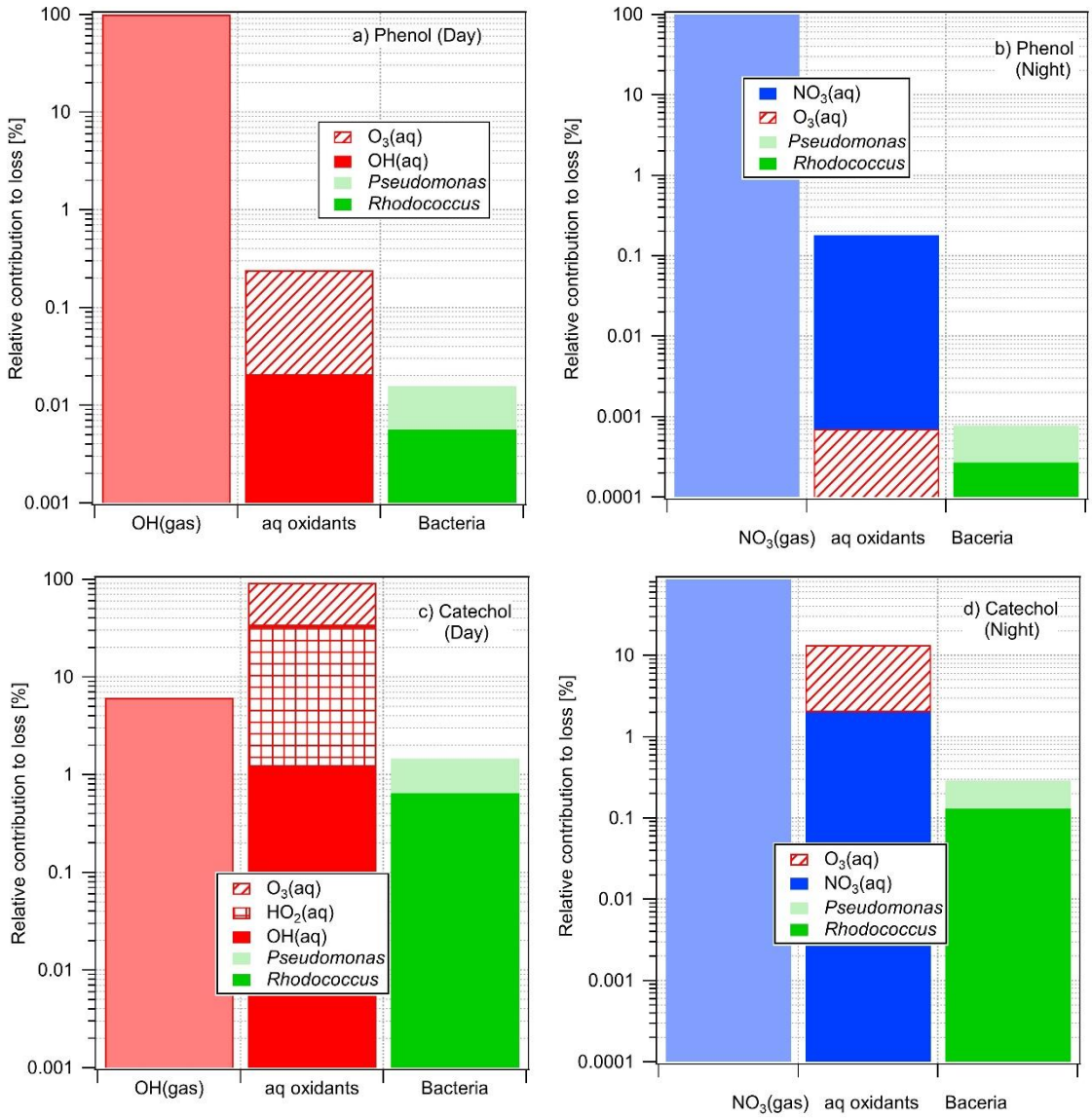


***Figure S- 3** : Relative contributions to total loss of phenol (a, b) and catechol (c, d) in the multiphase system including $HO_2^{\bullet}$ and $O_3$ reactions in the aqueous phase (Table S-3).*

**References**


Arakaki, T., Anastasio, C., Kuroki, Y., Nakajima, H., Okada, K., Kotani, Y., Handa, D., Azechi, S., Kimura, T., Tsuhako, A. and Miyagi, Y.: A general scavenging rate constant for reaction of hydroxyl radical with organic carbon in atmospheric waters, Env. Sci Technol, 47(15), 8196–8203, doi:10.1021/es401927b, 2013.

Berndt, T. and Böge, O.: Gas-phase reaction of OH radicals with benzene: products and mechanism, Phys. Chem. Chem. Phys., 3(22), 4946–4956, 2001.

Bielski, B. H. J., Cabell, D. E., Arudi, R. L. and Ross, A., . B.: Reactivity of HO2/O2- radicals in aqueous solution, J Phys Chem Ref Data, 14(4), 1041–1100, 1985.

Bolzacchini, E., Bruschi, M., Hjorth, J., Meinardi, S., Orlandi, M., Rindone, B. and Rosenbohm, E.: Gas-Phase Reaction of Phenol with NO3, Environ. Sci. Technol., 35(9), 1791–1797, doi:10.1021/es001290m, 2001.

Ervens, B., George, C., Williams, J. E., Buxton, G. V., Salmon, G. A., Bydder, M., Wilkinson, F., Dentener, F., Mirabel, P., Wolke, R. and Herrmann, H.: CAPRAM2.4 (MODAC mechanism): An extended and condensed

tropospheric aqueous phase mechanism and its application, J Geophys Res, 108(D14), 4426, doi:doi: 10.1029/2002JD002202, 2003.

Exner, M., Herrmann, H. and Zellner, R.: Laser-based studies of reactions of the nitrate radical in aqueous solution, Berichte Bunsenges Phys Chem, 96, 470–477, 1992.

Feigenbrugel, V., Le Calvé, S., Mirabel, P. and Louis, F.: Henry's law constant measurements for phenol, o-, m-, and p-cresol as a function of temperature, Atmos. Environ., 38(33), 5577–5588, doi:10.1016/j.atmosenv.2004.06.025, 2004.

Gurol, M. D. and Nekouinaini, S.: Kinetic behavior of ozone in aqueous solutions of substituted phenols, Ind. Eng. Chem. Fundam., 23(1), 54–60, doi:10.1021/i100013a011, 1984.

Hinteregger, C., Leitner, R., Loidl, M., Ferschl, A. and Streichsbier, F.: Degradation of phenol and phenolic compounds by Pseudomonas putida EKII, Appl. Microbiol. Biotechnol., 37(2), 252–259, doi:10.1007/BF00178180, 1992.

Hoffmann, E. H., Tilgner, A., Wolke, R., BÃ¶ge, O., Walter, A. and Herrmann, H.: Oxidation of substituted aromatic hydrocarbons in the tropospheric aqueous phase: kinetic mechanism development and modelling, Phys. Chem. Chem. Phys., 20(16), 10960–10977, doi:10.1039/C7CP08576A, 2018.

Hoigné, J. and Bader, H.: Rate constants of reactions of ozone with organic and inorganic compounds in water—I: Non-dissociating organic compounds, Water Res., 17(2), 173–183, doi:10.1016/0043-1354(83)90098-2, 1983.

Kläning, U. K., Sehested, K. and Holcman, J.: Standard Gibbs energy of formation of the hydroxyl radical in aqueous solution. Rate constants for the reaction $ClO_2^- + O_3 = O_3^- + ClO_2$, J Phys Chem, 89, 760–763, 1985.

Lallement, A., Besaury, L., Tixier, E., Sancelme, M., Amato, P., Vinatier, V., Canet, I., Polyakova, O. V., Artaev, V. B., Lebedev, A. T., Deguillaume, L., Mailhot, G. and Delort, A.-M.: Potential for phenol biodegradation in cloud waters, Biogeosciences, 15(18), 5733–5744, doi:10.5194/bg-15-5733-2018, 2018.

Lebedev, A. T., Polyakova, O. V., Mazur, D. M., Artaev, V. B., Canet, I., Lallement, A., Vaïtilingom, M., Deguillaume, L. and Delort, A.-M.: Detection of semi-volatile compounds in cloud waters by GC×GC-TOF-MS. Evidence of phenols and phthalates as priority pollutants, Environ. Pollut., 241, 616–625, doi:10.1016/j.envpol.2018.05.089, 2018.

Olariu, R. I., Barnes, I., Becker, K. H. and Klotz, B.: Rate coefficients for the gas-phase reaction of OH radicals with selected dihydroxybenzenes and benzoquinones, Int. J. Chem. Kinet., 32(11), 696–702, doi:10.1002/1097-4601(2000)32:11<696::AID-KIN5>3.0.CO;2-N, 2000.

Olariu, R. I., Bejan, I., Barnes, I., Klotz, B., Becker, K. H. and Wirtz, K.: Rate Coefficients for the Gas-Phase Reaction of NO3 Radicals with Selected Dihydroxybenzenes, Int. J. Chem. Kinet., 577–583, 2004.

Razika, B., Abbes, B., Messaoud, C. and Soufi, K.: Phenol and Benzoic Acid Degradation by Pseudomonas aeruginosa, J. Water Resour. Prot., 788–791, 2010.

Rudich, Y., Talukdar, R. K., Fox, R. W. and Ravishankara, A. R.: Reactive Uptake of NO3 on pure Water and Ionic Solutions, J Geophys Res, 101, 21023–21031, 1996.

Sander, R.: Compilation of Henry's law constants (version 4.0) for water as solvent, Atmos Chem Phys, 15(8), 4399–4981, doi:10.5194/acp-15-4399-2015, 2015.

Umschlag, T., Zellner, R. and Herrmann, H.: Laser-based studies of NO3 radical reactions with selected aroamtic compounds in aqueous solution, Phys Chem Chem Phys, 4, 2975–2982, 2002.

Zellner, R. and Herrmann, H.: Free Radical Chemistry of the Aqueous Atmospheric Phase, in Advances in Spectroscopy, vol. 24, edited by R. J. H. Clark and R. E. Hester, pp. 381–451, Wiley, London., 1994.